UCLA Samueli School of Engineering

Fast Track

SURP 2021

UCLA SAMUELI SUMMER UNDERGRADUATE RESEARCH PROGRAM

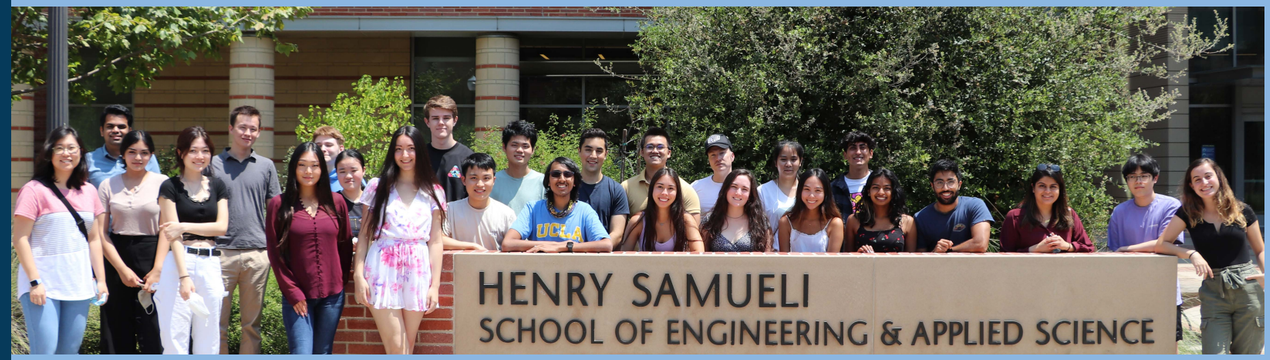

CONTENTS

DEAN'S MESSAGE

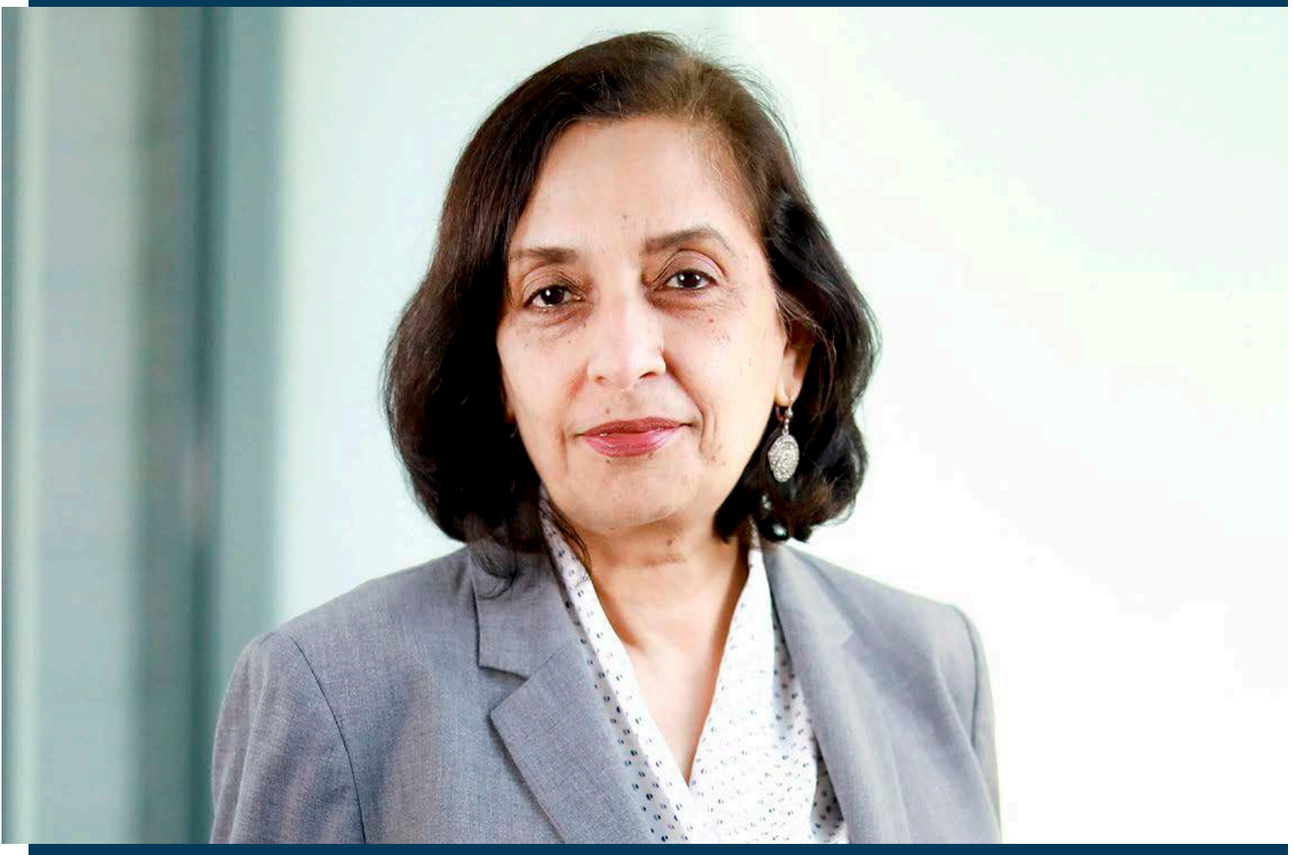

Ronald and Valerie Sugar Dean

The Summer Undergraduate Research Program (SURP) provides an intensive summer research experience in a wide range of engineering and physical science fields. Undergraduate students from all walks of life participate in research with UCLA Samueli School of Engineering faculty to gain real-world lab experience.

Due to the COVID-19 pandemic that is still affecting us this summer, SURP has had to transition the program into a remote learning environment for many of its scholars. Despite this challenge, SURP's many scaffolding resources and social events have still been able to occur and students were able to:

- Conduct research in a cutting-edge field at a world-renowned research institution.
- Meet and network with a community of peers who have similar goals and interests.
- Create a professional scientific poster and publish a research abstract.
- Learn to communicate research outcomes and present a detailed Summary of Project.
- Gain a competitive advantage for engineering graduate schools.
- Learn how you can impact your community as an engineer.

This year, a record 66 undergraduate students were selected to join the 2021 SURP cohort, spread out across 31 faculty in 6 engineering departments. We are happy to announce 64% of these are women, 20% are underrepresented minorities, and many are first generation and low income students. SURP is involved with ongoing efforts in fostering a more diverse, equitable and inclusive community at UCLA Samueli Engineering.

Creating new knowledge is a very difficult yet important task, and these high-performing students have done an outstanding job working through the rigors of academic research. These students should be very proud of all that they have accomplished in a short time this summer. I encourage you to explore our publication and learn about all the cutting-edge knowledge that is being created here.

Sincerely,

Dr. Jayathi Murthy
Ronald and Valerie Sugar Dean

Julia Bi

Electrical Engineering
Freshman, UCLA

Autonomous Vehicle with Offloaded Server Control using Mobile Edge Computing

FACULTY ADVISOR
C.K. Ken Yang

DAILY LAB SUPERVISOR
Jack Irish

DEPARTMENT
Electrical and Computer Engineering

ABSTRACT

Modern day mobile applications not only require a low latency, but but also incur a high energy cost. However, mobile devices are limited in their battery life and computational capabilities. Mobile Edge Computing (MEC) reduces latency and energy consumption by offloading some or all of the computing tasks to MEC servers. The Mobile Edge Compute Applications (MECA) lab establishes a 5G development environment that allows for experiments and testing with the 5G network and MEC. This particular project is an autonomous car controller which offloads control decisions to a central server, using a camera as input. Using gRPC, the camera sends images to the central server, which processes them and returns a control signal to guide the car. The goal is to compare the latency of this setup with traditional autonomous car controllers and achieve similar or better performance. At the moment, since it is difficult to gain access to physical materials, a simulation that imitates the complexity of video processing was used to gather data on the effectiveness of this strategy. As expected, sending the processing to a server is more time consuming with simple tasks, due to the initial time cost associated with the server-client communication. With more complex tasks, the server processing time is faster than processing at the client, since the server has better computational capabilities. The next step is applying these concepts to a physical setup with proper video processing and a car which takes the control signal.

UCLA Samueli School of Engineering

Autonomous Vehicle with Offloaded Server Control Using Mobile Edge Computing

Julia Bi, Jack Irish, Professor C.K. Ken Yang
Department of Electrical and Computer Engineering, University of California – Los Angeles

UCLA Samueli School of Engineering
SUMMER UNDERGRADUATE RESEARCH PROGRAM

Samueli Research Scholars
UCLA Samueli School of Engineering

FAST TRACK TO SUCCESS
UCLA Electrical and Computer Engineering

Introduction

The project aims to test concepts of Mobile Edge Computing (MEC), a technology that reduces latency and energy consumption of mobile devices through offloading computing tasks to external servers. Specifically, this concept was applied to an autonomous car that offloads decisions to a central server.

The goal is to measure the performance and latency of this setup, and compare it to traditional autonomous car controllers. We hypothesize that using MEC will allow the offloaded controller to have similar or better performance.

Background

Modern day mobile applications not only require a low latency, but also incur a high energy cost. However, mobile devices are limited in their battery life and computational capabilities.

Figure 1: Mobile Edge Computing (MEC) solves this issue by offloading some or all of the computing tasks to MEC servers at the edges of mobile networks, therefore improving efficiency and reducing latency.

This project is an autonomous car controller which, instead of making decisions on the car itself like traditional controllers, offloads control decisions to a central server, which becomes more efficient as the computations become more complex. The car uses a camera as input. It streams video to the central server, which processes the video and returns a control signal.

Materials and Methods

Client-Server Communication:

To communicate between the camera, server, and car, the project uses gRPC. gRPC is Google's open source RPC (Remote Procedure Call) system that allows for bidirectional messages as well as streaming.

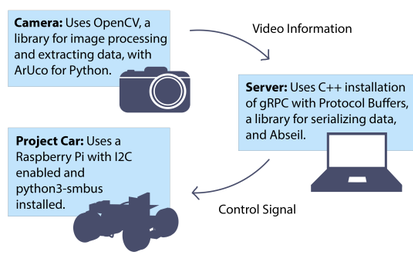

"Standard" Setup: The camera does the image processing and sends its results to the server, which then sends the results to the car. The image processing time is included in the camera-server latency.
"Streaming" Setup: The camera streams video directly to the server, which processes it and sends the result to the car. The image processing time is included in the server-car latency.

Results and Discussion

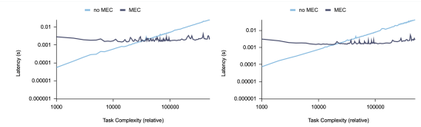

Figure 2: Task Complexity v. Latency Plots. Two simulations that imitate the complexity of video processing were used to gather data. As expected, server processing is more time consuming with simple tasks, due to the initial time cost of communication. With more complex tasks, the server processing time is faster because it has better computational capabilities.

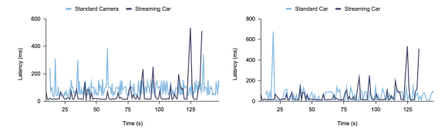

Figure 3: Time v. Latency Plots. *Left Plot:* The camera-server latency for the Standard setup and the server-car latency for the Streaming setup, both of which include the video processing, are plotted. The Streaming latency is on average lower than the Standard Latency by 39.2 ms, since the server has better computational capabilities. *Right Plot:* The server-car latencies for both the Standard and Streaming setup are plotted. The average latencies are roughly equal (Standard: 55.8 ms, Streaming: 49.3 ms), which is unexpected, since while their baseline latencies should be similar, the Streaming setup should be slightly slower on average because of the time taken by the server to do the image processing.

Conclusion

The relative efficiency of MEC vs Non-MEC in the simulation trials is as expected and confirms theory. The relative efficiency in the camera-car trials is somewhat unexpected and unclear, and should be investigated further.

Future Steps:

1. Further refine camera-car systems to stabilize latency measurements.
2. Gather and analyze data to explain unexpected results and confirm trends.

References

Gu, Xiaohui et al. "Energy-Optimal Latency-Constrained Application Offloading in Mobile-Edge Computing." Sensors (Basel, Switzerland) vol. 20,11 3064. 28 May. 2020, doi:10.3390/s20113064 https://pubmed.ncbi.nlm.nih.gov/32481742/

Mobile Edge Compute Applications Laboratory. https://mecalab.seas.ucla.edu

gRPC. https://grpc.io

Acknowledgements

I would like to thank Professor Yang and the MECA Lab, as well as the Samueli Engineering Summer Undergraduate Research Program and the Fast Track Program, for the support and resources. Many thanks to Jack Irish for his guidance and framework for this project. Many thanks to the Samueli Research Scholars Program for funding this research.

Sophia Du

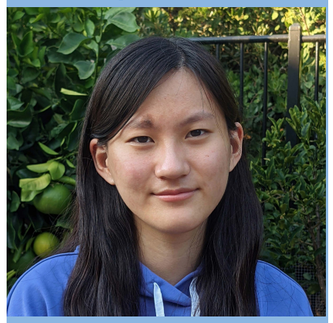

Electrical Engineering
Freshman, UCLA

Thermal Limitations of Miniature Printed Circuit Board (PCB) Photon Sources

FACULTY ADVISOR
Rob Candler

DAILY LAB SUPERVISOR
Benjamin Pound

DEPARTMENT
Electrical and Computer Engineering

ABSTRACT

Modern-day x-ray light sources use relativistic electron beams to produce photons. Quadrupoles and undulators are magnetic devices that form an integral part of these light sources. Current quadrupole and undulator technology at the micro to millimeter scale use electromagnets and are fabricated on silicon wafers. The objective of this research project is to explore the usage of printed circuit boards (PCBs) in quadrupoles and undulators and to test their limitations. PCBs could potentially make the current fabrication process of these devices easier and cheaper. However, PCB-based devices cannot reach the same current densities as silicon-based ones due to heating; the thermal conductivity of FR4, the PCB material, is significantly lower than that of silicon. Four designs (1 quadrupole, 3 undulators) with 1 to 2 trace layers were created in DipTrace and manufactured. COMSOL simulations showed that the four designs could run at current densities from 2.1×10 8 to 2.7×10 8 A/m2 before the FR4 reaches its glass transition temperature (130°C). Experimental data obtained with a thermal camera agreed reasonably well with the simulated data. The simulations and experiments both demonstrated that wider copper traces and more trace layers reduce temperature rise for the same total current but increase temperature rise for the same current density. Initial magnetic simulations of the quadrupole show that the quadrupole design can produce a magnetic gradient up to 34 T/m at the maximum experimental current density and 100 µm gap size. Future works include using active cooling systems to increase thermal performance and conducting real-world magnetic tests with the PCB designs.

UCLA Samueli School of Engineering

Thermal Limitations of Miniature Printed Circuit Board (PCB) Photon Sources

Sophia Du, Benjamin Pound, Rob Candler
Sensors and Technology Laboratory (STL), Department of Electrical and Computer Engineering, University of California - Los Angeles

FAST TRACK TO SUCCESS
UCLA Electrical and Computer Engineering

UCLA Samueli School of Engineering
SUMMER UNDERGRADUATE RESEARCH PROGRAM
STL

Introduction

Modern x-ray light sources, like x-ray free electron lasers and synchrotrons, use relativistic electron beams to produce photons. Quadrupoles and undulators are magnetic devices that form an integral part of these light sources.

Quadrupole — a magnet that focuses the electron beam on one axis and defocuses it on the other. Multiple quadrupoles can be placed in succession with a 90° rotational offset for focusing in both dimensions.

Undulator — alternating dipole magnets that accelerate electrons transverse to their direction of travel in a periodic manner; this causes the electrons to generate photons. The wavelength of the photons depends on the spacing of the dipole magnets, or the undulator period, and the electron velocity.

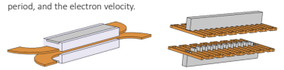

Figure 1: Miniature Panofsky Quadrupole (left) and Serpentine Design Undulator (right) [1]

Current quadrupole and undulator technology at the micrometer to millimeter scale use electromagnets produced on silicon wafers. Electric currents that produce magnetic fields flow through copper traces (orange). Magnetic yokes (dark gray), material with high magnetic permeability, increase the magnetic field strength.

PCB Designs

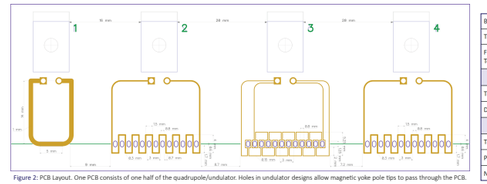

Figure 2: PCB Layout. One PCB consists of one half of the quadrupole/undulator. Holes in undulator designs allow magnetic yoke pole tips to pass through the PCB.

Table 1: Design Specifications

Board Dimensions	37 × 102 × 0.8 mm
Trace Thickness	2 oz (70 µm)
FR4 Transition Temperature	130 - 140 °C
Quadrupole	
Trace Width	1 mm
Device Length	5 mm
Undulator (serpentine, coil)	
Trace Width	0.3 mm, 0.15 mm
Period	3 mm, 3 mm
Number of Periods	6.5, 6

Table 2: Design Descriptions

#	Device	Design	Layers
1	Quadrupole	Miniature Panofsky	1
2	Undulator	Serpentine	1
3	Undulator	Coil	2
4	Undulator	Serpentine	2

- serpentine design undulator — the copper traces wind around the holes.
- coil design undulator — the copper traces closely wrap around each hole.
- two layers — copper traces are on the top and bottom of the PCB, increasing current capacity.

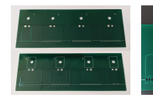

Figure 3: PCB Front and Back

Figure 4: PCB Size Comparison

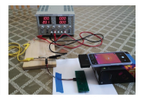

Figure 5: Experiment Setup

Objectives

1. Design printed circuit boards (PCBs) for quadrupoles and undulators used in miniature photon sources.
2. Test the current and thermal limitations of the PCBs.

Advantages

✓ Fabrication of copper traces on a PCB is easier and cheaper than fabrication with silicon substrates; this can reduce costs significantly, increasing the accessibility of compact light sources.
✓ Multiple quadrupoles and undulators can be placed on one PCB and aligned before manufacturing.

Disadvantages

✗ FR4, the material of the PCB, has a low thermal conductivity compared to silicon. Heat generated by the high currents flowing through the copper traces will dissipate slowly, which can lead to the PCB overheating.
✗ Due to lower currents, PCB-based devices produce weaker magnetic fields compared to silicon-based devices.

Methods

1. Design PCBs for multiple quadrupoles and undulators — DipTrace
2. Find current limits of copper traces for each design using industry standards — IPC
3. Perform thermal simulations of designs — COMSOL
4. Test manufactured PCBs and measure temperature with thermal camera

Results

Table 3: Maximum current capacity based on the IPC-2152 industry standard [2]

IPC-2152 Standard Maximum Current Capacity	
ambient temperature = 25°C temperature increase = 25°C external trace layer	
Design	Current Per Trace (A)
1	4.68
2	2.34
3	1.57
4	2.34

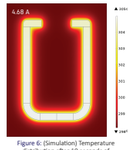

Figure 6: (Simulation) Temperature distribution after 10 seconds of continuous current, Design 1.

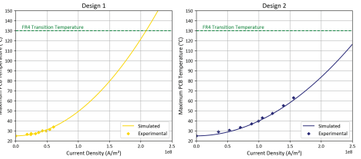

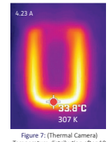

Figure 7: (Thermal Camera) Temperature distribution after 10 seconds of continuous current, Design 1. Hottest point is marked.

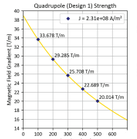

Figure 8: Quadrupole (Design 1) magnetic field gradient vs. gap size.

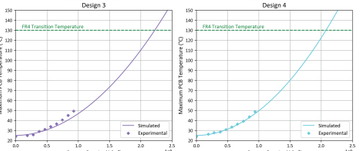

Figure 9: Maximum temperature after 10 seconds of continuous current vs. current density for each design. Lines denote simulated data and diamonds denote experimental data.

Conclusion & Future Works

- Simulated data agreed reasonably well with experimental data.
- Wider copper traces and more trace layers reduce temperature rise for the same total current but increase temperature rise for the same current density.

- Perform magnetic simulations and real-world tests with the designs.
- Test the PCB's thermal performance with pulsed current and with active cooling systems.
- Design PCBs with more than 2 trace layers to utilize internal layers.

References

[1] Pound, B. A. (2021). Micro and Milliscale Magnetic Systems for Particle Beam Manipulation [Prospectus].
[2] Sierra Circuits. (2021). PCB trace width, Current capacity and Temperature rise calculator. twcalculator.app.protoexpress.com.

Acknowledgements

I would like to thank Professor Rob Candler for giving me the opportunity to work in his lab and Ben Pound for his guidance throughout my research project. I also would like to thank the National Science Foundation, the UCLA Summer Undergraduate Research Program, and the UCLA ECE Fast Track to Success Program.

Nicholas Hamakami

Electrical Engineering
Freshman, UCLA

Evaluation of Network Topologies in Challenging Environments

FACULTY ADVISOR
Christina Fragouli

DAILY LAB SUPERVISOR
Mine Dogan

DEPARTMENT
Electrical and Computer Engineering

ABSTRACT

Finding the optimal network topology for wireless sensor networks is an important problem that has a wide variety of applications in the field of environmental and earth sensing. This is because issues with connectivity and routing can arise if the environment a topology is in contains obstacles that impede the communication between nodes – examples of such environments being towns or cities. As such, our research focuses on synthesizing wireless sensor networks that satisfy certain sensing and communications requirements in these challenging environments. Towards this end, we created occupancy grids based on satellite images that display the locations of obstacles and free space. For different placements of sensor nodes on the occupancy grids, we assessed the performance of the resulting networks based on our sensing requirements and the maximum flow that can be sent from a source to a destination. The data that we collected will be the basis for a new algorithm that can determine effective sensor network topologies for high-obstacle environments.

Evaluation of Network Topologies in Challenging Environments

Nicholas Hamakami, Mine Dogan, Christina Fragouli

Department of Electrical and Computer Engineering, University of California – Los Angeles

FAST TRACK TO SUCCESS
UCLA Electrical and Computer Engineering

UCLA Samueli School of Engineering
SUMMER UNDERGRADUATE RESEARCH PROGRAM

Introduction

Context:
Finding the optimal network topology for wireless sensor networks is an important problem because issues with connectivity and routing can arise if the environment a topology is in contains obstacles that impede communication between nodes.

Main goals:
- Optimize a sensor network topology in a difficult environment – e.g., city or neighborhood – using occupancy grids and minimum cuts
- Criterion: Maximize the network flow rate for a given network

Motivation:
- Sensor networks have a wide variety of applications in environmental and earth sensing
- Need data as a foundation for a new algorithm that can determine effective topologies in high-obstacle environments

Materials

Google Maps API
- Occupancy grid creation

Python
- Occupancy grid creation
- Node placement with sensing constraints
- Calculations: link capacities, minimum cuts

NumPy

Methods

Create occupancy maps with the Google Maps API and other image editing software. Then transform maps into proper grids with Python.

Google Maps image (left) to occupancy image (right)

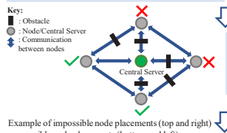

Input occupancy grids into algorithm to determine node placements based on constraints of distance and line of sight.

Example of impossible node placements (top and right) vs. possible node placements (bottom and left).

Find channel coefficients for each pair of nodes through the channel coefficient equation.

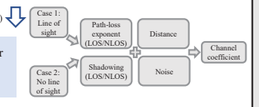

Link capacity equation:

$$L = \log(1 + P|h|^2)$$

Key:
L: Link capacity
P: Transmission power
h: Channel coefficient

Channel coefficients: Subsume the effects of distance, shadowing, and path-loss at a reference distance of 1 meter

Link capacities: Measurement of how much data can be sent through a link between two nodes

Calculate link capacities based on channel coefficients through the link capacity equation.

Water analogy:
Higher link capacity synonymous with higher water flow

Low (left) vs. high (right) link capacity

Use finalized link capacities to calculate minimum cuts – and thus maximum network flow – through the Gomory-Hu Tree Algorithm.

Gomory-Hu Tree Algorithm: Takes in link capacities and returns a Gomory-Hu tree. To find a minimum cut for a pair of nodes from the Gomory-Hu tree, find the smallest edge on the path between the nodes.

Node Placement Algorithm

Choosing a selection of nodes that meet sensing constraints:

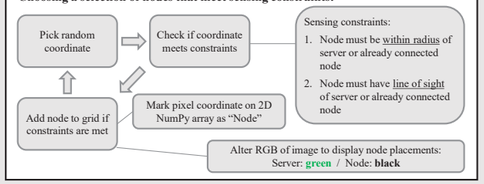

Results

Example satellite image to network flow process:
Location: UCLA – Manning, Malcom, La Conte Ave intersection

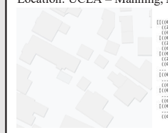

Input: Google Maps satellite image

Figure 1: Occupancy grid represented as a 2D NumPy array. Each coordinate is marked as either "Occupied," "Not Occupied," or "Node"

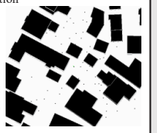

Figure 2: Final distribution of 50 nodes and a single central server

Key observations:
- Vast majority of nodes were placed either near the central server or in an open area where there is access to other nodes
- As expected, few nodes were placed near the edge of the grid

Calculating the maximum network flow from minimum cuts:
- Minimum cuts – act as a restrictor to the maximum flow. In other words, the flow of a network can only be as large as its minimum cut
- Flow rate given in unambiguous units of flow

Conclusion

Next steps – data collection:
Our next objective is to use this algorithm to create node distributions for a variety of maps, with the main goal being to compare the network flow of the different maps.

Closing thoughts:
Having created a method to generate node distributions and quantifiably measure their effectiveness, we are one step closer to our end goal of developing an algorithm that can determine effective network topologies for high-obstacle environments.

References

Gomory, Ralph E., and Tien Chung Hu. "Multi-terminal network flows." *Journal of the Society for Industrial and Applied Mathematics* 9.4 (1961): 551-570.

Acknowledgements

I would like to thank Professor Christina Fragouli, the Summer Undergraduate Research Program, the Fast Track to Success Program, and the National Science Foundation for the opportunity to conduct this research. I would also like the thank William Herrera, Mine Dogan, and Jonathon Bunton for their continued support throughout the program.

Bhavik Joshi

Computer Engineering
Freshman, UCLA

Multi-Hop Mesh Networking with Frequency Diversity as Robust Communication Infrastructure for Robotic Swarms

FACULTY ADVISOR
Ankur Mehta

DAILY LAB SUPERVISOR
Ankur Mehta

DEPARTMENT
Electrical and Computer Engineering

ABSTRACT

Robotic swarms are groups of autonomous robots that work together in order to perform tasks through cooperative behavior and interactivity with their environments. In order for robotic swarms to collaborate, they must have a reliable way of communicating with one another. Thus, we created a robust network infrastructure to allow autonomous robots to work together through peer-to-peer communication even in difficult environments. As a means of doing so, we used the painlessMesh Arduino library to implement a multi-hop mesh network, or a network topology that allows each node to relay signals to nodes too far away by routing packets across intermediate nodes. Additionally, we added 433 MHz packet radios onto our hardware stack and sent each message between robots over multiple, distinct frequencies; this keeps interference on one frequency band from preventing successful communication. Through this infrastructure, we enabled our robots to successfully communicate with any other robot. We also saw that for certain messages, when one frequency became unusable, our diversity maintained the infrastructure's ability to communicate reliably. In the future, this work can be used to bring robotic swarms one step closer to becoming ubiquitous and useful in daily life, improving their communication so that together they can accomplish tasks previously and independently impossible.

UCLA Samueli School of Engineering

Multi-Hop Mesh Networking with Frequency Diversity as Robust Communication Infrastructure for Robotic Swarms

LEMUR

Bhavik Joshi, Dr. Ankur Mehta, The Laboratory for Embedded Machines and Ubiquitous Robots, UCLA

FAST TRACK TO SUCCESS
UCLA Electrical and Computer Engineering

UCLA Samueli School of Engineering
SUMMER UNDERGRADUATE RESEARCH PROGRAM

Objective

We are creating a **robust network infrastructure** with a multi-hop mesh network and frequency diversity for robotic swarms to communicate over.

Goal:
- Robots can communicate, even in difficult environments

Robotic Swarms:
- Collaborative robots
- Environment interactivity
- Must communicate reliably

Infrastructure Elements

Hardware used:

ESP32 Featherboard, 433 MHz Packet Radio

Software used:
- painlessMesh
  - Mesh over WiFi
- Radiohead library
- Arduino IDE

Network Nodes

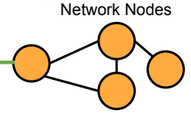

We created a software package that implements:
- 433 MHz radio into a multi-hop mesh network
- A bridge node that relays packets between an external network and other nodes
- Swarm communication into a simple to use Arduino library

Network Robustness

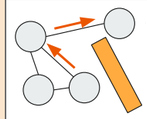

Multi-Hop Mesh Network:
- Any node to any node
- Intermediates relay signals to unreachables

↓

Why: to allow our robots to **communicate with any other** robot

Frequency Diversity
- Using multiple, distinct frequencies (2.4 GHz and 433 MHz)

↓

Why: our robots **communicate over both** so interference on one doesn't stop communication

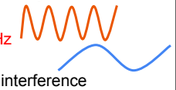

Results and Conclusions

The network enabled our robot swarms to:
- Work autonomously
- Respond to commands

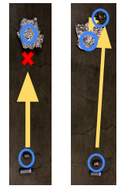

Effect of a 433 MHz Jammer on Packets Received Over Multiple Frequencies

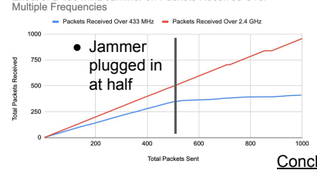

- Jammer plugged in at half

Because of the reflective obstacle, the signal has to hop across nodes

The network is robust:
- Works when one frequency fails
- Indirect nodes can communicate

Conclusions and Future

This research advances swarm communication

↓

Swarms can do harder tasks in more difficult environments

↓

Robotic swarms become ubiquitous

Acknowledgements

- William Herrera, Summer Undergraduate Research Program
- Dr. Ankur Mehta, Grace Kwak, Jaehoon Song, Jillian Pantig, Marisa Duran, Shahrul Kamil Hassan, and Sudarshan Seshadri, UCLA Lemur

Kim Kha

Mathematics
Junior, Mount Saint Mary's

Enoch Huang

Electrical Engineering
Freshman, UCLA

Amanda Hacker

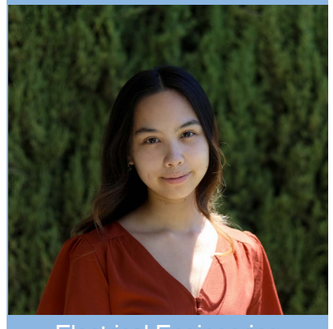

Electrical Engineering
Freshman, UCLA

Wearable & Mobile Bioanalytical Technologies for Personalized Medicine

FACULTY ADVISOR
Sam Emaminejad

DAILY LAB SUPERVISOR
Hannaneh Hojaiji

DEPARTMENT
Electrical and Computer Engineering

ABSTRACT

Exponential growth in Internet of Things (IoT) devices and wearable sensing technologies has created an unprecedented opportunity to enable personalized medicine through real-time individual biomonitoring. Although these commercialized platforms are capable of tracking physical activities and vital signs, they fail to access molecular-level biomarker information which provide insight into the body's dynamic chemistry. Thus, as sweat is a rich source of biomarkers that can be retrieved unobtrusively, sweat-based wearable biomonitoring has emerged as one of the most promising candidates to merge this gap. By designing and integrating compact electrochemical sensors into wearable electronic devices, we can non-invasively and accurately track specific biomarkers in sweat and provide actionable feedback about users' health status. We develop a signal modulation strategy to stimulate our electrochemical sensors for wearable biomarker monitoring. We also design a novel sensor readout methodology for improved and accurate biomarker tracking. Then, we integrate these designs into a wireless electrochemical readout circuitry to noninvasively track intended biomarkers. As a result, we successfully demonstrate our signal modulation solution's efficacy through electrodeposition of prussian blue films. Additionally, we show this sensing methodology improves signal readout and sensitivity by 3 times. Thus, we can non-invasively track subjects' biomarkers and underlying health status in a wireless and wearable format. This platform can further be utilized for real-time glucose monitoring in diabetic patients without requiring conventional painful extraction methods, or monitoring lithium levels in bipolar patients for drug abuse/compliance.

Wearable & Mobile Bioanalytical Technologies for Personalized Medicine

Amanda H. Hacker[1], Enoch I. Huang[1], Kim T. Kha[2], Hannaneh Hojaiji[1] and Sam Emaminejad[1]

[1]Department of Electrical Engineering, University of California, Los Angeles
[2]Department of Physical Science & Mathematics, Mount Saint Mary's University

FAST TRACK TO SUCCESS
UCLA Electrical and Computer Engineering

UCLA Samueli School of Engineering
SUMMER UNDERGRADUATE RESEARCH PROGRAM

INTRODUCTION

The exponential growth in Internet of Things (IoT) devices and wearable sensing technologies have created an unprecedented opportunity to enable personalized medicine.

Although commercialized IoT devices and wearable sensors are capable of tracking physical activities and vital signs, they fail to access molecular-level biomarker information that provide insight into the body's dynamic chemistry.

Sweat-based wearable biomonitoring has since emerged as one of the most promising candidates because sweat is a rich source of biomarkers that can be retrieved unobtrusively[1]. However, a series of wearable sensors and electronic systems need to be designed to provide access to these biomarkers and realize wearable sweat sensing.

OBJECTIVES

1. Define a signal modulation strategy to stimulate our electrochemical sensors for wearable biomarker monitoring.
2. Develop a novel sensor readout methodology for improved and accurate biomarker tracking.

TECHNICAL TERMS

Near Field Communication (NFC): Inductive coupling between a reader and a tag
Cyclic Voltammetry (CV): Detect the electrochemical properties of biomarkers at the sensor for accurate sensing.

PRINCIPLES

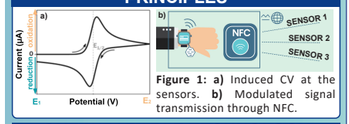

Figure 1: a) Induced CV at the sensors. **b)** Modulated signal transmission through NFC.

OUR WEARABLE TECHNOLOGY

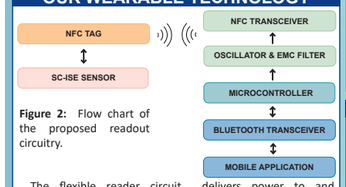

Figure 2: Flow chart of the proposed readout circuitry.

The flexible reader circuit delivers power to and communicates with the flexible tag on the skin. The circuitry of the tag then rectifies the modulated signal to scan the sensors.

MATERIALS

Circuit Simulation: LTSpice, Microsoft Excel
Sensor & System Development: Lithium (Li) solutions, Li Ion-Selective-Electrodes (ISE sensors), a commercial potentiostat, custom-developed flexible printed circuit board (FPCB), and electronic components.

METHOD FOR SENSOR TESTING

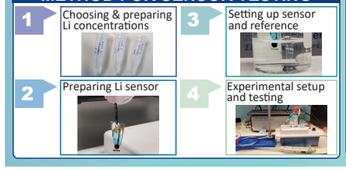

CIRCUIT SIMULATION PROCESS

1. Oscillator, EMC filter, match network characterizations
2. Evaluate the signals at different nodes
3. Use Excel to plot the amplitude modulated signal

SENSOR STIMULATION METHODS

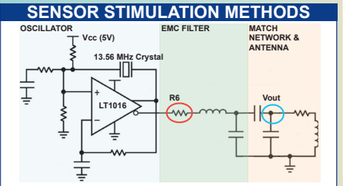

Figure 3: Signal modulation circuitry generating a spectrum of sine waves at 13.56 Mhz.

To realize the waveform for CV, we specifically designed the circuit to modulate voltages for analyte detection.

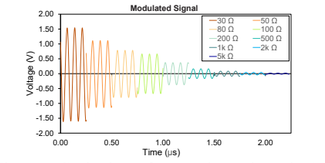

Figure 4: Simulated waveform at the reader showing effect of programming a trimmer at the EMC filter on modulating and generating the intended waveform.

Accordingly, we can modify the reader to demonstrate the accuracy and application of our design.

SENSOR DEVELOPMENT

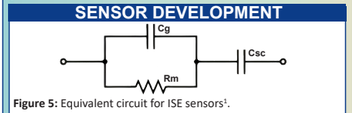

Figure 5: Equivalent circuit for ISE sensors[1].

ISE Sensor Technical Terms:
Rm: solution resistance
Cg: geometric capacitance of the electrode
Csc: fabricated sensor's capacitance
ISE: acts as a transducer which converts ion activity into electric potential for biomarker sensing

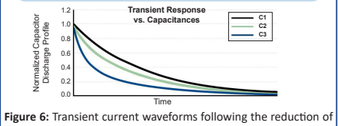

Figure 6: Transient current waveforms following the reduction of the internal capacitance.

We utilize ISE sensors to perform biomarker sensing in sweat and in a wearable format. Understanding of the equivalent circuit portrays how the sensor works and interacts with the tag.

The sensors demonstrate a transient response due to the internal capacitance of the sensor (Csc) causing shift in the readout signal.

By adding an external real capacitance in the circuit we can suppress this transient response and stabilize sensor measurement, decreasing potential drift.

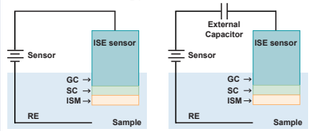

Figure 7: Circuit diagram of ISE with added capacitance.

As demonstrated in Fig. 6, by incorporating a real capacitance into the circuit, we can reduce the internal capacitance of the sensor for improved and accurate sensing results.

RESULTS

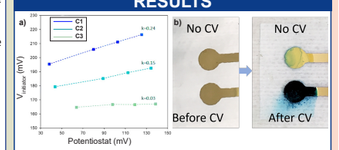

Figure 8: Results for **a)** improved sensor signal readout method and **b)** effective signal modulation.

We observed improved sensitivity in Li readouts by manipulating the internal electrochemical capacitance of the ISE sensor and successfully deposited Prussian Blue on the gold electrode as an indication of correct application of CV amplitude modulation by the circuit.

CONCLUSION & FUTURE WORK

1. Achieved wireless CV scanning of sensors enabling active biomarker sensing in a series of electrochemical sensors.
2. Improved the tag's sensitivity to current drifts of ISE sensors through specific adjustment of internal capacitance.

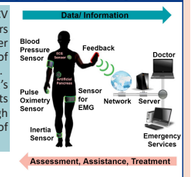

This system can further be utilized to track and monitor biomarker profiles in biological media and enable a tracking systems for the healthcare system to realize personalized medicine.

REFERENCES

[1] Emaminejad, Sam, et al. "Autonomous sweat extraction and analysis applied to cystic fibrosis and glucose monitoring using a fully integrated wearable platform." PNAS (2017): 201701740.

ACKNOWLEDGEMENTS

We would like to thank the National Science Foundation for funding our project through the UCLA Summer Undergraduate Research Program. Additionally, we would like to thank Professor Emaminejad, our PhD student advisor Hannaneh Hojaiji for her advice and support, and Will Herrera for his guidance throughout the research program.

Krisha Minocha

Computer Engineering
Freshman, UCLA

Camera-based Heart Rate Estimation Focused on Mitigating Bias

FACULTY ADVISOR

Achuta Kadambi

DAILY LAB SUPERVISOR

Pradyumna Chari

DEPARTMENT

Electrical and Computer Engineering

ABSTRACT

The COVID-19 pandemic has led to an influx of telehealth appointments, causing difficulty in assessing vital signs virtually. Our work focuses on remote photoplethysmography (R-PPG), the concept of measuring heart rate using color fluctuations in the face. Many different algorithms already exist with varying levels of success; however, one major gap is the lack of performance of these existing algorithms on darker skin tones, which, given the prevalence of cardiovascular disease in African American communities, creates a pressing issue. We have employed a VGG-style convolutional network known as DeepPhys to learn different spatial masks and increase robustness across the board. My work has focused on improving this existing network to increase medical accuracy by manipulating the structure of the network along with training parameters.

UCLA Samueli School of Engineering

Camera-based Heart Rate Estimation Focused on Mitigating Bias

Krisha Minocha, Pradyumna Chari, Professor Achuta Kadambi
Department of Electrical and Computer Engineering - UCLA

Introduction

There has recently been a notable influx in telehealth visits due to the COVID-19 pandemic. While telehealth has created a way to provide patient care remotely, it is extremely difficult to assess vital signs such as heart rate, breathing rate, etc., indicating that there is clearly a need for contactless heart rate sensing solutions. While there are existing computer vision solutions available, they exhibit a bias against darker skin tones.

Key Concepts

Remote Photoplethysmography (R-PPG)
- Type of algorithm focused on using subtle color variations in the face to measure a blood volume pulse and, consequently, estimate heart rate.

Convolutional Neural Network
- A computer system modeled on the human brain and nervous system, specifically focused on mimicking the optic nerve and image processing

Objective

I aim to implement an improved computer vision model for measuring heart rate using deep learning. My goal is to increase performance specifically on darker skin tones.

VITAL Dataset

Vital-sign Imaging for Telemedicine AppLications developed by Visual Machines Group at UCLA
- At least 432 videos of 54 subjects
- Focus on a diverse dataset in terms of gender, race, age, skin tone, etc.
- Using two different camera angles and four different lighting conditions with only a smartphone camera

I will be working to train the algorithm on this dataset in order to ensure optimal performance across the board.

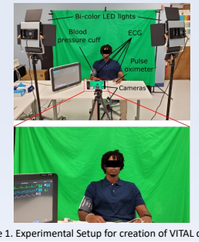

Figure 1. Experimental Setup for creation of VITAL dataset

Proposed Algorithm

My proposed algorithm will build of off the existing DeepPhys algorithm developed by W. Chen and D. McDuff consisting of:
- A VGG-Style Convolutional Neural Network (up to 19 layers)
- Learns spatial masks for regions of interest to maximize performance and robustness
- Emphasis on diffuse component, ignoring the mirror-like reflections of the skin
- Uses two streams: Motion and Appearance in order to maximize performance

This algorithm was able to improve performance with motion and talking. However, there is still a bias in terms of skin tone. My proposed changes will be to the structure of the model to hopefully improve performance across the board. I plan on doing this by using different activation and loss functions and observing the results.

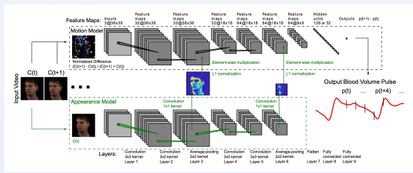

Figure 2. Proposed Algorithm Structure Using Both Appearance and Motion Streams to Increase Robustness

Conclusion and Results

Activation/Loss Function Combination	Mean Absolute Error (bpm)
rrelu/softmarginloss	18
tanh/MSE	13.166
selu/pearson	12.73
relu/MSE	12.57
relu/L!Loss	12.57
rrelu/MSE	11.257
rrelu/L1Loss	11.257
rrelu/pearson	11.251

Table 1. Table of experimental results of loss/activation function manipulation

This work furthers previous algorithmic advances such as the existing DeepPhys algorithm to increase accuracy. We can see that regardless of loss function, the rrelu activation function creates the best results. However, there is still a large margin of error, which needs to be corrected. This work can also be extended outside of the medical realm into reducing bias in other computer vision applications such as facial recognition, etc.

References

1. Chari, Pradyumna, et al. "Diverse R-PPG: Camera-Based Heart Rate Estimation for Diverse Subject Skin-Tones and Scenes." *ArXiv*, 2020. https://arxiv.org/pdf/2010.12769.pdf
2. Chen, Weixuan, and Daniel McDuff. "DeepPhys: Video-Based Physiological Measurement Using Convolutional Attention Networks." *ArXiv*, 2018, https://arxiv.org/pdf/1805.07888.pdf

Acknowledgements

We would like to thank the UCLA Summer Undergraduate Research Program for organizing this research internship and the Samueli Research Scholars Program for funding it. We would also like to thank the UCLA Fast Track to Success Electrical and Computer Engineering Program for their continued guidance and support. I would also like to thank Pradyumna and Professor Kadambi for challenging me and creating such a supportive and creative atmosphere for learning.

Aadhidhya Ravikumar

Electrical Engineering
Freshman, UCLA

Jenna Kim

Electrical Engineering
Freshman, UCLA

Deep Learning Approaches for Transmitter Classification

FACULTY ADVISOR

Danijela Cabric

DAILY LAB SUPERVISOR

Danijela Cabric

DEPARTMENT

Electrical and Computer Engineering

ABSTRACT

Wireless signal classification plays an important role in the security of a wireless communication system since it can be used for transmitter authorization, the process by which authorized transmitters are distinguished from non-authorized transmitters based on transmitter-specific traits in their signals. Current systems have only investigated authorization for a closed set scenario, where the algorithm classifies among a finite set of known transmitters. This has several limitations, the most significant of which is that transmitters outside of the known set may be misclassified. In this project, we attempt to remedy this issue by performing authentication in an open set scenario, where the number of transmitters is not known. To do this, we generated and transmitted signals from eleven different ADALM Pluto Software Defined Radios using MATLAB software. We also simulated 5 unique transmitters by artificially adding different I/Q imbalance impairments to the signals. The signals were transmitted in the form of packets (active transmission separated by idle moments), which were then extracted using pre-written code. Finally, the extracted packets were inputted into an existing deep learning algorithm called One Vs. All, where the algorithm was tested and modified until a satisfactory accuracy was found. With this algorithm, wireless communication security can be significantly improved, since it minimizes the risk of misclassification by solving the previous weakness of authorization only under closed set conditions.

UCLA Samueli School of Engineering
SUMMER UNDERGRADUATE RESEARCH PROGRAM
FAST TRACK TO SUCCESS
UCLA Electrical and Computer Engineering

Deep Learning Approaches for Transmitter Classification

Jenna Kim, Aadhidhya Ravikumar, Professor Danijela Cabric

Department of Electrical and Computer Engineering, University of California, Los Angeles

UCLA CORES
NSF

INTRODUCTION

Wireless communication requires a **transmitter** to generate and transmit signals. For security purposes, it is important to be able to differentiate between transmitters to ensure that only authorized signals are received. This is known as **classification**.

Previous research has only approached classification in a closed set scenario, where a classifier classifies among a finite set of known transmitters. When transmitters outside of the known set are introduced, misclassification may occur, which could result in severe security threats.

A more useful and versatile method would be to classify in an **open set** scenario, where the chance of misclassification is greatly reduced because the number of transmitters is not known beforehand.

OBJECTIVE

DEFINITION:
Deep learning is a subset of machine learning that mimics the neural networks of a human mind. It can be used to process data in order to make decisions.

To improve wireless communication **security** through **transmitter classification** in an **open set**. We hypothesize that this can be accomplished using a **deep learning algorithm**.

REFERENCES

[1] Hanna, Samer, et al. "Deep Learning Approaches for Open Set Wireless Transmitter Authorization." 2020 IEEE 21st International Workshop on Signal Processing Advances in Wireless Communications (SPAWC), 2020, doi:10.1109/spawc48557.2020.9154254

ACKNOWLEDGEMENTS

We would like to thank Professor Danijela Cabric for her support and guidance throughout this project, as well as Samurdhi Karunaratne for his help and resources. We would like to thank the National Science Foundation (NSF) for providing funding and the UCLA Summer Undergraduate Research Program for granting us this opportunity.

METHODS

Signals were generated, transmitted, and received from **ADALM-Pluto Software Defined Radios** using **MATLAB** software. The algorithm was built and tested using **python** in **Google Colaboratory** notebooks.

STEP ONE → STEP TWO → STEP THREE

DATA COLLECTION

- Generate & transmit WiFi signals from 15 transmitters in calm channel conditions (ie. no interference)
- Receive signals using 1 transmitter

Figure 1: Example of the waveform of a received WiFi signal, transmitted over regular intervals.

DATA CONVERSION

- Extract periods of active signal (packets) from the received signals
- Convert data from a .mat file to a .pkl file

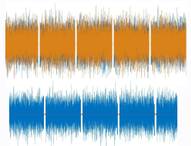

Figure 2: Waveform of a received signal with extracted packets.

TEST ALGORITHM

- Input .pkl file into the One Vs. All algorithm
- Reduce number of authorized transmitters and known outliers
- Adjust regularizers until program performs adequately

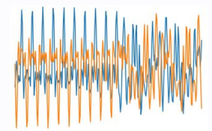

Figure 3: Example of the waveform of an authorized signal.

RESULTS & DISCUSSION

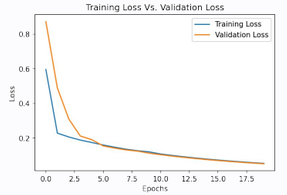

Figure 4: Graph of training loss versus validation loss for a set of 15 transmitters, with 3 authorized transmitters and 6 known outliers. Ideally, we wish to see minimal gapping between the two plots. Thus, the algorithm performed very well, with an accuracy of 0.94 and a chance of misclassification of 0.002.

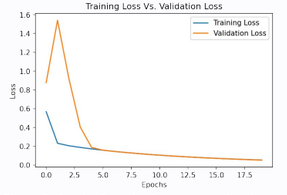

Figure 5: Graph of training loss versus validation loss with an increased number of authorized transmitters (5) and a decreased number of known outliers (5). The accuracy was found to be 0.91, and chance of misclassification was 0.003.

CONCLUSIONS

Our results and the performance of the OvA classifier show the effect of multiple transmitters under calm channel conditions on the classification of authorized and non-authorized transmitters, thus displaying the potential to classify and protect against unknown threats.

In a wider scope, we have shown that deep learning methods can successfully perform transmitter authentication. This is one of the first instances of classification performed under open set conditions; it opens the door for future advances in securing open sets.

FUTURE PROSPECTS

IMPROVE — Optimize efficiency by **reducing the time required to train** before a sufficient result is achieved.

EXPAND — Increase versatility by modifying the algorithm to work for **any number of transmitters.**

APPLY — **Implement** algorithm in a wireless communications system and run algorithm with **real-world signals**.

Nicolas Schmidt

Electrical Engineering
Junior, UCLA

Terahertz polarization imaging using quantum-cascade laser with switchable polarization

FACULTY ADVISOR

Benjamin Williams

DAILY LAB SUPERVISOR

Anthony Kim

DEPARTMENT

Electrical and Computer Engineering

ABSTRACT

We are using a terahertz quantum-cascade vertical external cavity surface emitting laser (QC-VECSEL) with switchable polarization for polarization difference imaging. Terahertz radiation's non-damaging nature gives it several applications such as cancer detection, bomb detection, and drug detection. Furthermore, polarimetric imaging can show various features not shown by traditional images, such as roughness, edge details, and birefringence. To optimize imaging, we first found the focal point of the laser, meaning where the gaussian beam spot size is minimum. Next, we investigated the signal to noise ratio through a wide range of parameters. We found the parameters with the strongest signal to noise ratio and from there we could move on to imaging. The beam goes through a biconvex lens, the sample, a rotating polarizer and finally two off-axis parabolic mirrors focus it onto the detector. Then we use Stokes-Mueller formalism to conveniently model the partially polarized light. Our images suggest that polarization difference can show edge features with high contrast for samples transparent in the terahertz frequency range.

UCLA Samueli School of Engineering

UCLA Samueli Electrical & Computer Engineering

Terahertz polarization imaging using quantum-cascade laser with switchable polarization

Nicolas Schmidt[1], Anthony D. Kim[1], Benjamin S. Williams[1]
[1]Department of Electrical and Computer Engineering, University of California Los Angeles (UCLA), Los Angeles, CA 90095

Terahertz Devices and Intersubband Nanostructures Laboratory

Introduction

- **Terahertz (THz) radiation** is able to penetrate through a wide range of non-metals. Furthermore, due to its low energy it is known to cause no detectable damage to matter.
- **THz imaging** shows promise in medicine (cancer detection), security (illegal drug and bomb detection), agriculture (water content detection) and more.
- Imaging via polarization can show various features not shown by traditional images. It is significantly more sensitive than conventional imaging, showing features such as **roughness, edge details, and birefringence**.

Terahertz illumination

- **We use a teraquantum-cascade (QC) vertical-external-cavity surface-emitting-laser (VECSEL) with switchable polarization.**
- Our laser uses a metasurface with two different arrays of antennae and quantum-cascade gain which are respectively activated via an electrical bias.
- The two sets have quasi-orthogonal linear polarizations with set 1 emitting a beam at about 45° and set 2 at about 135°. The two sets also show excellent beam quality.
- We operate our QC-VECSEL at operating temperature 77K, 10% duty cycle, at 3.2 THz, 0.7mW average power for the top set and 0.5 mW for the bottom set

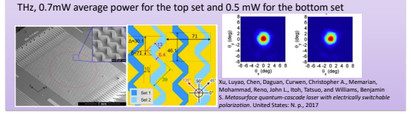

Xu, Liuyao, Chen, Daguan, Curwen, Christopher A., Memarian, Mohammad, Reno, John L., Itoh, Tatsuo, and Williams, Benjamin S. *Metasurface quantum-cascade laser with electrically switchable polarization*. United States: N. p., 2017

Experimental setup and detection methods

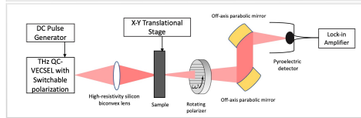

Diagram of optical setup.

- **The pulsed QC-VECSEL with linear polarization goes through a high-resistivity silicon biconvex lens to be focused onto a sample.**
- **The THz signal coming out of the sample is modulated a linear polarizer rotating at 10 Hz.**
- Lock-in amplifier collects the in-phase and quadrature component of the laser beam, which can be used to calculate the polarization state of the beam after going through the sample.
- We use Stokes-Mueller formalism to analyze the light reaching the detector.

Resolution and noise

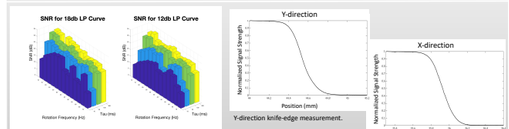

SNR testing results.

- 100 samples of the laser are taken while variating the rotating polarizer's frequency, the lock-in amplifier's averaging time (tau) and the frequency the lock-in amplifier uses for the signal (double the rotation frequency).
- Optimal operation parameters for the optical setup are found to, 10 Hz rotation frequency, resulting in a 20 Hz lock-in frequency, and tau of 300ms

- Using knife-edge measurements with the X-Y translational stage we measure the diameter of the focal point of the beam to be $\mathbf{0.28}\ \boldsymbol{mm}$ in both the X and Y direction.
- This measurement corresponds to the transmission drop from 90% to 10% of the laser's maximum transmission

Stokes-Mueller Formalism

- Stokes-Mueller formalism is convenient to model the partially polarized light coming out of our sample

$$\boldsymbol{S} = \begin{pmatrix} S_0 \\ S_1 \\ S_2 \\ S_3 \end{pmatrix} = \begin{pmatrix} \langle E_x^2 \rangle + \langle E_y^2 \rangle = \langle I_{0^\circ} \rangle + \langle I_{90^\circ} \rangle \\ \langle E_x^2 \rangle - \langle E_y^2 \rangle = \langle I_{0^\circ} \rangle - \langle I_{90^\circ} \rangle \\ 2\langle E_x E_y \cos\left(\delta_y(t) - \delta_x(t)\right)\rangle = \langle I_{45^\circ} \rangle - \langle I_{135^\circ} \rangle \\ 2\langle E_x E_y \sin\left(\delta_y(t) - \delta_x(t)\right)\rangle = \langle I_{LC} \rangle - \langle I_{RC} \rangle \end{pmatrix}$$

- Furthermore, our rotator and lock-in amplifier system provides the Stokes parameters.

$$\boldsymbol{M_{rotator}} = \frac{1}{2}\begin{pmatrix} 1 & \cos(2\omega t) & \sin(2\omega t) & 0 \\ \cos(2\omega t) & \cos^2(2\omega t) & \sin(2\omega t)\cos(2\omega t) & 0 \\ \sin(2\omega t) & \sin(2\omega t)\cos(2\omega t) & \sin^2(2\omega t) & 0 \\ 0 & 0 & 0 & 0 \end{pmatrix}$$

- With this we can extract the intensity and the change from the initial polarization-angle at the edges and features of the sample.
- Intensity:

$$S_{out,1} = \frac{1}{2}(S_0 + S_1\cos(2\omega t) + S_2\sin(2\omega t))$$

- Polarization Angle:

$$\psi_{rot} = \frac{1}{2}\tan^{-1}\left(\frac{S_2}{S_1}\right)$$

Results

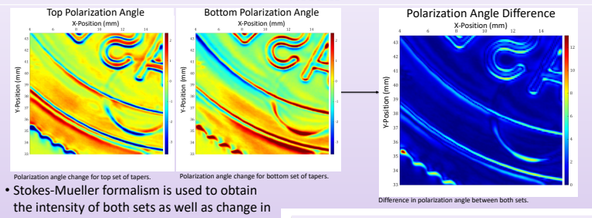

- Stokes-Mueller formalism is used to obtain the intensity of both sets as well as change in polarization angle of the laser.
- It can be seen by analyzing these images that the orthogonal polarizations show different features more prominently. It is of interest to consolidate these features into one image.
- The clearest image obtained from this specific sample was the difference in polarization angle, as all the features of the sample are most clearly seen.
- It is clear to see the features such as the edges and roughness of the sample

Conclusion

- Our resultant images suggest polarization difference imaging can resolve edge features with high contrast for objects transparent in the terahertz frequency such as plastic

Future Prospects:

- Splitting the initial beam to compare the intensity measured through the sample to the intensity to the full intensity without going through through the sample.
- Vary the optical setup to capture information such as reflection.

Acknowledgements

- Funding support is provided by the National Science Foundation (NSF).

Sudarshan Seshadri

Electrical Engineering
Freshman, UCLA

Gathering and Presenting Sensor and Control Data from Autonomous Agents, Interpreting High Level User Behavior Inputs

FACULTY ADVISOR

Ankur Mehta

DAILY LAB SUPERVISOR

Ankur Mehta

DEPARTMENT

Electrical and Computer Engineering

ABSTRACT

A successful user interface for a group of autonomous robots must have three main characteristics. First, it must be able to easily gather and visualize data as well as send commands to the robotic swarm. Second, because robotic projects constantly evolve, it must be highly modular and display data in many formats. Lastly, it must be able to replay the data as if in real time, which previous systems, such as typical IoT dashboards, cannot do. We were able to create a demo of a swarm of robots that feature mesh networking, autonomy, and vision processing. Using the front end JavaScript library React, I created a dashboard that is able to transfer data over different protocols as well as record data to play back later. I implemented different input methods such as text boxes, sliders, joysticks, and buttons. Members of my lab can now easily visualize robot data in different ways including video feeds, raw text feeds, live graphs, and 3D rotation visualization. Ultimately this project enables users to easily prototype and control a generic swarm of robots. In the event that new controls or interfaces are needed, the modularity of this project makes it easy to implement new functionality.

Assisted Autonomy Dashboard

Gathering and Presenting Sensor and Control Data from Autonomous Agents, Interpreting High Level User Behavior Inputs

Sudarshan Seshadri, Dr. Ankur Mehta,
The Laboratory for Embedded Machines and Ubiquitous Robots, UCLA

LEMUR
UCLA Samueli School of Engineering
SUMMER UNDERGRADUATE RESEARCH PROGRAM
FAST TRACK TO SUCCESS
UCLA Electrical and Computer Engineering
NSF

Introduction

A successful user interface for controlling a group of robots must:

- Gather and visualize data from multiple sources and sinks
- Be highly modular: any part can be replaced
- Record data for playback, to compare robot runs

Web App Structure

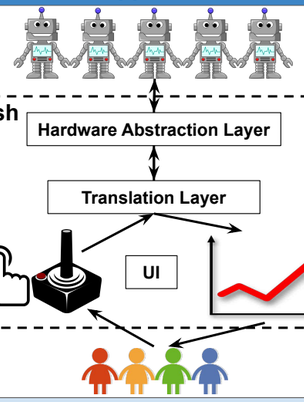

- Split into several parts to increase modularity.
- Each component can be swapped out for an alternative.

Conclusion

- Control any group of robots.
- Add new controls and data visualization elements easily (modularity)
- Future developments:
  - add more input and output components
  - add more troubleshooting/prototyping tools
  - integrate into RoCo (origami robot design tool)

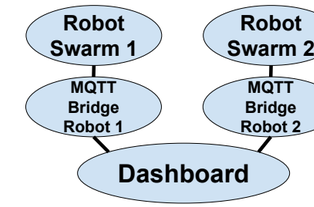

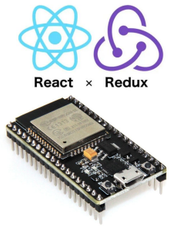

Results

The dash can control boats, cars, Blimps, any new robots developed.

Input Components:

- Text
- Buttons
- Joysticks
- Macros
- Sliders

Display Components:

- Text
- Rotation Display
- Video
- Graphs

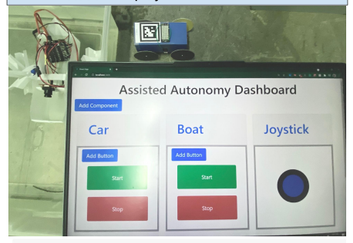

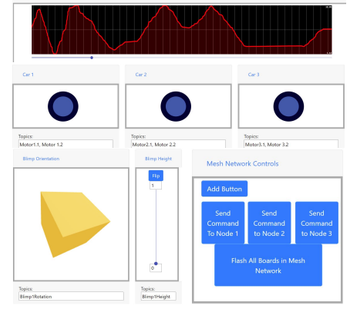

Protocols

- Websockets
  - Full duplex over TCP
  - HTTP initiates connection
- MQTT
  - Publish / subscribe
  - Broker / clients

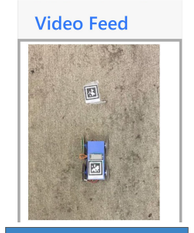

Acknowledgements

- Dr. Ankur Mehta, UCLA LEMUR
- Grace Kwak, Jaehoon Song, Bhavik Joshi, Jillian Pantig, Marisa Duran, Shahrul Kamil Hassan
- William Herrera, Summer Undergraduate Research Program

Krish Shah

Computer Engineering
Freshman, UCLA

Waree Protprommart

Biochemistry
Sophomore, Mount Saint
Mary's University

William Clark

Computer Science
Sophomore, Los Angeles City College

Expanding Human-Computer Interaction via Object Recognition Implemented into a Hand Signal Actuated Robotic Arm (SARA)

FACULTY ADVISOR

Xiang 'Anthony' Chen

DAILY LAB SUPERVISOR

Jiahao Li

DEPARTMENT

Electrical and Computer Engineering

ABSTRACT

Human-computer interaction (HCI) has advanced the efficacy of a multitude of sectors such as communication and consumerism. However, there exists a gap where most HCI research is conducted to improve quality in industrial aspects rather than personal aspects. Our research extends HCI to improve quality of life by designing and implementing a hand signal response AI into a six degree of freedom (6DoF) robotic arm. We call this our hand signal actuated robotic arm, SARA. An implementation of forward kinematics (FK) and inverse kinematics (IK) in python allows the robotic arm to actuate in response to complex hand signals, made possible via our hand recognition software. This software presents a real-time object-tracking process that recognizes hand signals by finger landmark mapping. A rule classifier distinguishes different variations of raised fingers. To confirm mechanical actuation and limitations, we developed a simulator in MATLAB using a virtual robotic arm that parallels SARA. Our research ultimately produced a design that, when implemented, gives SARA the capability to react to diverse hand signals independently. Qualitative demos conducted with a variety of hand signals validated our research design and implementation. A set of thirty-two hand signals was displayed to SARA that resulted in successful actuation in accordance with the simulator. The application of this design aims to assist individuals with physical limitations, making HCI more personal. The success of implementing a hand signal response AI makes the interaction with a robotic arm intuitive, ultimately expanding the scope of HCI to enhance the human experience.

Joonwoo Shin

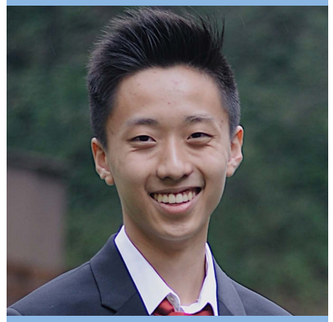

Electrical Engineering
Freshman, UCLA

Viterbi Algorithm for Decoding TCM based PAS

FACULTY ADVISOR

Richard Wesel

DAILY LAB SUPERVISORS

Dan Song, Linfang Wang

DEPARTMENT

Electrical and Computer Engineering

ABSTRACT

The development of a trellis-coded modulation (TCM) based probabilistic amplitude shaping (PAS) coding scheme has the potential to greatly improve the rate of data transmissions to meet the rapidly growing data demands. Previous studies on convolutional codes have determined that there is a theoretical maximum channel noise in the memoryless channels used for data transmission; a TCM based PAS design has the potential to reach a higher maximum threshold in comparison to low-density parity-check (LDPC) codes. To obtain the initial data sequence, we propose an implementation of the maximum likelihood soft decision Viterbi algorithm that calculates the branch metrics using a probability vector for the constellation design in order to determine the survivor path.

Viterbi Algorithm for Decoding TCM based PAS

Joonwoo Shin, Felipce Areces, Dan Song, Linfang Wang, and Richard Wesel

Department of Electrical and Computer Engineering,
University of California, Los Angeles

Fast Track to SUCCESS summer scholars program
Electrical Engineering Department

Introduction

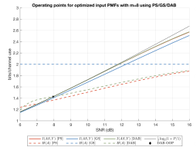

Figure 1. *Theoretical performance limit.*

- **Problem:** There is a theoretical maximum noise threshold in the memoryless channels used for data transmission that has not been achieved at short block lengths.
- **Approach:** Using a nonuniform input and a Trellis-coded modulation (TCM) based Probabilistic amplitude shaping (PAS) system may approach this theoretical limit.
- **This Project:** Implement the maximum likelihood soft decision Viterbi algorithm to determine the original transmitted data from the received data sequence.
- **Significance:** This work seeks to increase the speed and reliability of short transmissions.

Trellis Coded Modulation

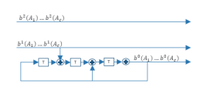

Figure 2. *Rate 2/3 Convolutional Encoder. Two uncoded bits enter the encoder. One input bit is uncoded and does not affect the state of the encoder, and the remaining bit is processed into two coded bits. The T boxes represent the states of the shift register. The + represents an XOR notch that process any two bits.*

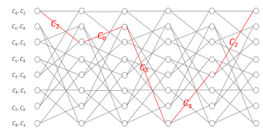

Figure 3. *Trellis diagram of the convolution encoder in Figure 2. Each node indicates a unique state in the shift register. Each path between nodes represents the next possible states, depending on the input symbol. The red lines indicate an example path of encoder states over time. This trellis uses parallel branches.*

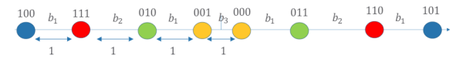

Figure 4. *Constellation diagram for the encoder in Figure 2. The first two bits represent the two coded bits outputted from the encoder. The third bit is the uncoded bit that passes through the encoder.*

- The convolutional encoder:
  - Creates a redundant bit for every 2 bits in the data sequence before transmission.
- The trellis:
  - Stores the next possible states from any given state and the coded output bits for any uncoded input bit.
  - Does not consider the uncoded bit that passes through the encoder.
  - Each path represents two parallel branches for the two possible uncoded bits that passed through the encoder.
- The constellation design:
  - Separates constellation points share two parallel branches, i.e. that differ only in an uncoded bit, to have the maximum possible distance.

Methods

- All code was implemented in MATLAB, using the Communications Toolbox.

MATLAB

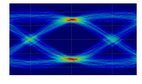

Soft Decision Viterbi Algorithm

- Viterbi Algorithm:
  - Cannot determine the original sequence with complete certainty.
  - Calculates most likely transmitted sequence given the received sequence.
  - The path through the trellis that has the highest probability is selected by the Viterbi algorithm.
- Soft Decision Decoding:
  - Calculates the path metric of each path through the trellis using a priori probabilities of the input symbols, which are not equal in our design.
  - More reliable but also more computationally complex than hard decision decoding, which computes path metrics using Hamming distance.

Design

- Inputs:
  - Vector of encoded channel symbols.
  - Trellis corresponding to the encoder used.
  - Probability vector of the constellation design.
  - Vector of constellation points.
- Output:
  - Vector of decoded bits
- Implementation:
  - Starting from the zero state, traverse each next possible state in the trellis.
  - Calculate the squared Euclidean distance and sum the new path metric for each branch.
  - For converging paths, discard the branch with the greater path metric.
  - Store the input symbols, paths choices, and path metrics of each state in the trellis.
  - Select path having the highest probability, i.e. smallest path metric.
  - Return the sequence of input symbols reshaped as a vector of bits.

Conclusion and Future Work

- The TCM based PAS coding scheme has the potential to greatly improve the rate of data transmissions.
- Examples: performance benefits in any digital video, radio, or mobile communication systems.
- Prospects:
  - Further optimizations of decoder.
  - Translation to C++
  - Measure the performance of TCM based PAS system with this decoder.

Acknowledgements

We would like to thank the National Science Foundation, UCLA ECE Fast Track Program, and UCLA Summer Undergraduate Research Program for funding our project and providing the research opportunity. We would like to thank Professor Wesel, Dan Song, Linfang Wang, and Felipe Areces for the extensive guidance throughout the research process.

References

[1] Ungerboeck, G. (1982). Channel coding with multilevel/phase signals. *IEEE Transactions on Information Theory*, *28*(1), 55–67. https://doi.org/10.1109/tit.1982.1056454
[2] Xiao, D., Wang, L., Song, D., & Wesel, R. D. (2021). Finite-Support Capacity-Approaching distributions for Awgn channels. *2020 IEEE Information Theory Workshop (ITW)*. https://doi.org/10.1109/itw46852.2021.9457608
[3] Wesel, R. D. (2004). Reduced-State representations For Trellis codes Using CONSTELLATION SYMMETRY. *IEEE Transactions on Communications*, *52*(8), 1302–1310. https://doi.org/10.1109/tcomm.2004.833023

Esha Thota

Computer Engineering
Freshman, UCLA

Sraavya Pradeep

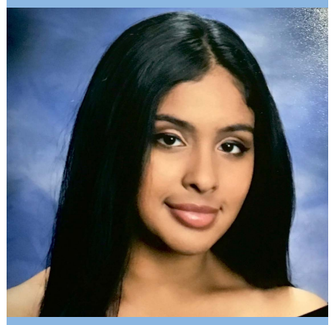

Computer Engineering
Freshman, UCLA

Low Complexity Algorithms for Transmission of Short Blocks over the BSC with Sparse Feedback

FACULTY ADVISOR

Richard Wesel

DAILY LAB SUPERVISOR

Amaael Antonini

DEPARTMENT

Electrical and Computer Engineering

ABSTRACT

Practically speaking, most communications channels are imperfect; noise will interfere with the communications and corrupt transmitted data. In order to combat this, many communications systems utilize feedback- the practice of relaying information regarding received data back to the transmitter- in order to efficiently transmit and decode messages. Research in this field, arguably set in motion by Michael Horstein in 1963, studies this phenomena and ways to mitigate interference. This research builds off an existing algorithm created by Amaael Antonini and Rita Gimelshein, which uses causal encoding over the the BSC (Binary Symmetric Channel), a channel through which binary messages can be transmitted with an equal crossover probability of zeros and ones. It modifies the algorithm to utilize sparse feedback instead of bitwise feedback- sending feedback after a specially determined number of bits have been sent through the channel, rather than after every bit, aiming to increase efficiency without loss in performance.

Low Complexity Algorithms for Transmission of Short Blocks over the BSC with Sparse Feedback

FAST TRACK TO SUCESS

Esha Thota, Sraavya Pradeep
PI: Richard Wesel, DLS: Amaael Antonini

CSL

UCLA Samueli School of Engineering
SUMMER UNDERGRADUATE RESEARCH PROGRAM

INTRODUCTION

Most communications channels are imperfect; noise will interfere and corrupt transmitted data. To combat this, communications systems relay information (regarding data sent to a receiver) back to the transmitter.

The current method uses causal encoding, which simultaneously transmits and verifies bits.

OBJECTIVE

New research modifies the algorithm to utilize sparse feedback: sending feedback after a determined number of bits have gone to the receiver, instead of every bit, to increase efficiency without loss in performance.

MATERIALS

- Matlab
- CLion Software
- GMP Library
- CLion

PARTITIONING

After systematic transmission, we must determine how many partitions we should use for the number of bits being transmitted. We do this by: log2((1-p)^k) Where p is the error probability of the channel, and k is the number of bits to be transmitted.

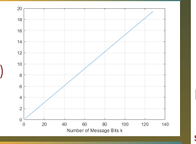

RESULTS

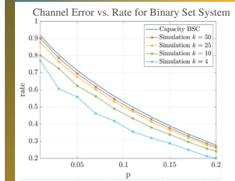

Figure 1. Regular Feedback System. ref. A. Antonini & R. Gimelshein

Regular Feedback System
The graph displays the error probability *p* of the channel against the performance rate (rate at which messages are transmitted & decoded) As the transmitted bits *k* increase, we approach performance closer to channel capacity.

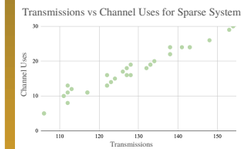

Figure 2. Sparse Feedback System

Sparse Feedback System
The graph displays the transmissions vs channel uses of the Sparse Feedback system. We see that as we increase the transmissions, the channel usage will increase. (Plot shown for block size 2, partition count 4)

SPARSE SYSTEM

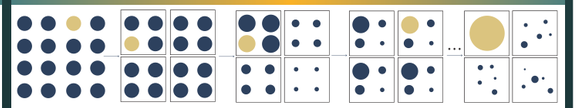

16-bit system; all messages have equal probability of being true. Receiver's belief state of each is 1/16. The true message in yellow.

Partition all messages into four sets with equal probability (S0, S1, S2, S3). Transmitter sends data about theta being in a set.

After some communication betweeen the transmitter & receiver, the probability of S0 has gone up, and other sets have gone down.

Rearrange messages within sets so probabilities of each set is close to equal. We then continue the process from steps 2 & 3.

After much repetition, the true message reaches a probability such that it is the only message contained in a set. We enter confirmation phase.

METHODS

Updating Probabilities.

Using **GMP library** for arbitrary precision + **Matlab** functionality. Modify the current algorithm to update & merge probabilities of multiple sets. First, recalculate multiple-way probabilities using **Bayes' Rule of Conditional Probability**, which is:

$$p(B \mid A) = \frac{p(A \mid B)\, p(B)}{p(A)}$$

Must use the error probability *p* and its complement *q*, aka (1-*p*), to calculate probability of the transmitted message.

Merging Probabilities.

We must store all messages with their probabilities in an ordered fashion, so we can later sort through them & partition appropriately. To do this, we place the message structs into an ordered linked list, ordering them by **decreasing probability**.

Regrouping The Sets.

Reorganize messages into determined number of sets with equal (or close to equal)probability. Use partition (see: sparse system) to organize groups by filling up each probability "bucket" (partition) to a value within tolerance of the **target probability**. Once message reaches a probability that exceeds a bucket's tolerance, we halve number of partitions.

CONCLUSION

Regular Feedback System

Binary Set system- splits all messages into one of two sets. Uses a version of ACK/NACK (Acknowledgement/Negative Acknowledgement) feedback to determine probability of theta.

- Pros: Simpler logic means less processing time/overhead
- Cons: Channel use is less efficient, bitwise transmission and decoding

Sparse Feedback System

Multiple Set system- finds the ideal number of partitions based on # of k bits. Splits probabilities into the "buckets". Uses more complicated logic to determine probability of theta from a message of multiple bits.

- Pros: Channel use decrease within certain range of tolerance, improved performance
- Cons: Limited range of improvement, overhead affected by extra processing

ACKNOWLEDGEMENTS

We would like to thank the National Science Foundation, UCLA Summer Undergraduate Research Program, and UCLA's Fast Track to Success for providing the resources for this publication. We would also like to thank Professor Richard Wesel, and Amaael Antonini for their guidance and support.

REFERENCES

Antonini, Rita G. and Richard Wesel. Causal (Progressive) Encoding over Binary Symmetric Channels with Noiseless Feedback, D1-S3-T1.2, ISIT 2021.

Brendan Towell

Electrical Engineering
Junior, UCLA

Ava Asmani

Electrical Engineering
Freshman, UCLA

High Rate Tail Biting List Decoder using a Dual Trellis

FACULTY ADVISOR

Richard Wesel

DAILY LAB SUPERVISOR

Beryl Sui

DEPARTMENT

Electrical and Computer Engineering

ABSTRACT

Encoders and decoders in communications systems are critical for the accurate and efficient transmission of information over noisy channels. Our research is focused on encoders and decoders for tail-biting convolutional codes used in conjunction with cyclic redundancy check (CRC) codes. We implement encoders and decoders that correct errors in the received message when possible. Often, when an error cannot be corrected, the CRC informs the decoder that the selected codeword is unreliable. In our research, we extend the work of Liang et al., who demonstrated that the use of distance spectrum optimal cyclic redundancy checks (DSO CRCs), along with list decoding, offered significant improvements in signal to noise ratio (SNR) with minimal additional computational cost for low rate convolutional codes of the form 1/n, which have n output bits for every 1 input bit. Our research applies this approach to high rate convolutional codes of the form (n – 1)/n, which have n output bits for every n – 1 input bits. Specifically, we implemented the decoder for a rate-3/4 tail-biting convolutional encoder, and used the dual trellis approach proposed by Yamada et al. for efficient decoding, along with the tree-trellis list decoding algorithm proposed by Roder and Hamzaoui. By implementing this system in C++, we have the ability to simulate its performance at low frame error rates and compare it to both the random coding union bound and the performance of a standard maximum likelihood decoder.

UCLA Samueli School of Engineering

SUMMER UNDERGRADUATE
RESEARCH PROGRAM

High Rate Tail-Biting List Decoder using a Dual Trellis

Ava Asmani, Brendan Towell, Wenhui Sui[1], Richard Wesel[2]
Communications Systems Laboratory, Department of Electrical and Computer Engineering
University of California, Los Angeles
[1]Daily Lab Supervisor, [2]Principal Investigator

Fast Track to SUCCESS summer scholars program
Electrical Engineering Department
UCLA Samueli School of Engineering

Introduction

- Transmitting data across noisy channels using high rate convolutional codes and standard maximum likelihood decoding on the encoder-based trellis incurs high decoding costs. To improve efficiency, we implement the dual trellis proposed in Yamada et al. [1], which is based on the parity check matrix of the original code, and improves efficiency for high rate decoding by reducing the number of comparisons performed at each state in the trellis.
- To improve robustness, we built off the work of Liang et al. [5], who demonstrated that for low rate convolutional codes (of the form 1/n), using distance spectrum optimal cyclic redundancy checks (DSO CRCs), in conjunction with serial list decoding, provided significant improvements to signal to noise ratio (SNR) at a fairly low cost.
- Our work extends this approach to high rate codes (of the form (n-1)/n), to identify if such an approach is viable for high rate codes as well.

Materials

We implemented the dual trellis list Viterbi algorithm with DSO CRCs in C++, and plotted the results in Matlab.

Methods

- We started by building the maximum likelihood high rate tail-biting decoder, then incorporated the dual trellis, and finally implemented list decoding.
- Fig. 1 on the right outlines the process of evaluating the system.
- For each SNR, we ran trials until we reached 200 frame errors, so our FER would have a statistically significant number of errors.

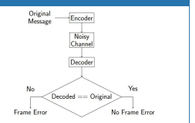

Figure 1: Evaluating performance of the system

Convolutional Codes

- Convolutional codes use memory elements in the encoding process to add redundancy to the encoded signal, which can be used to correct errors in the received message.
- Since the outputs are a function of the memory elements and inputs, this can be viewed as a state machine, which we can arrange on a trellis to account for multiple input blocks. For brevity, only one state transition is shown in Fig. 2.

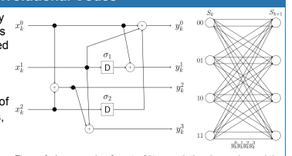

Figure 2: An example of a rate-3/4 convolutional encoder and the corresponding trellis. Each adder is modulo 2, so each value will remain a binary 1 or 0. This encoder has two memory elements, denoted by sigmas.

Dual Trellis

- For standard maximum likelihood decoding, we want to find the message closest to the received message by comparing all possible paths through the trellis, however, directly enumerating them all is computationally intractable.
- The Viterbi algorithm efficiently finds this sequence by only storing the locally optimal path at each state, upper bounding the number of paths to keep track of at the number of states.

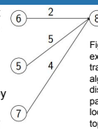

Figure 3: In this small example of one state transition, the Viterbi algorithm would discard the lower paths, since they are locally worse than the top path.

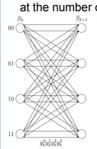

Figure 4: Standard (left) vs Dual Trellis (right)

- While highly efficient relative to the naive approach, the Viterbi algorithm on the standard trellis still struggles with high rate codes due to the high number of comparisons needed at each state.
- Using the dual trellis, which is based on the parity check matrix of the code, reduces the number of comparisons needed at each state, improving efficiency despite the larger number of states and state transitions.

List Decoding

- Adding DSO CRCs provides a further layer of redundancy to rule out invalid decoded messages.
- If a decoded message fails the CRC check, serial list decoding computes the next most likely path by using the paths that were more likely, but failed the CRC.
- The locally second best path will either be one divergence from one of the locally best paths, or a path corresponding to a different starting state, since more than one divergence will always add additional weight compared to one divergence on its own.
- This can be efficiently implemented by using a red-black binary search tree, as described by Röder and Hamzaoui [5].
- To cap decoding complexity, we fix the list size, which is the maximum number of messages that can be checked.

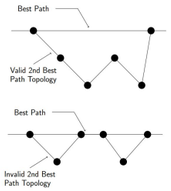

Figure 5: Valid and Invalid Next Best Path Topologies

Results

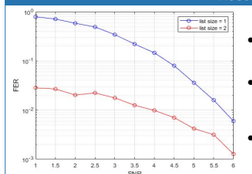

Figure 6: Frame error rate for list sizes of one and two, using the optimal rate-3/4 code with six memory elements, and a blocklength of 30 bits.

- As seen in Fig. 6, increasing list size offers significant improvements in FER for a given SNR.
- Use of the dual trellis reduced decoding complexity by 75% compared to the standard trellis for a rate-3/4 system with two memory elements.
- Larger list sizes produce less frame errors in the decoded message at the cost of increased decoding complexity.

Conclusion, Future Works, and Limitations

- The improvement to FER provided by the list decoding algorithm, with minor increases in decoding complexity, indicates that the method of using S-LVA with DSO CRC for low rate codes presented in Liang et al. [5] generalizes well to high rate codes.
- We're still working on the software implementation, so this poster only includes data for small list sizes. When fully implemented, we plan to test longer list sizes, as well as varying blocklengths and code rates.
- A high rate tail-biting list decoder using a dual trellis accurately and efficiently decodes transmitted data. However, information theory provides theoretical limits on the performance of any communication system, regardless of decoding complexity.

References

[1] Yamada, T. et al. "A New Maximum Likelihood Decoding of High Rate Convolutional Codes using a Trellis".
[2] Seshadri, N. and Sundberg, C.-E.W. "List Viterbi Decoding Algorithms with Applications".
[3] Yang, H. et al. "CRC-Aided List Decoding of Convolutional Codes in the Short Blocklength Regime".
[4] Röder, M. and Hamzaoui, R. "Fast Tree-Trellis List Viterbi Decoding".
[5] Liang, E. et al. "List-Decoded Tail-Biting Convolutional Codes with Distance-Spectrum Optimal CRCS for 5G".

Acknowledgements

We would like to thank Dean Wesel for his guidance and leadership throughout the research process. We are grateful to the National Science Foundation for funding, through the Summer Undergraduate Research Program and the UCLA Electrical and Computer Engineering Department. Finally, we would like to thank Beryl Sui, Hengjie Yang, Linfang Wang, and Ethan Liang for their assistance with the technical aspects of our project.

Tyler Xu

Electrical Engineering
Freshman, UCLA

A Personalized Approach to Federated Learning

FACULTY ADVISOR

Suhas Diggavi

DAILY LAB SUPERVISOR

Kaan Özkara

DEPARTMENT

Electrical and Computer Engineering

ABSTRACT

Federated learning, a machine learning technique, has been gaining popularity as a method of protecting user data privacy for modern-day devices while still providing a great user experience by only sending model updates to the server instead of exchanging sensitive data. However, utilizing a singular global model is extremely restricting as the data is exceedingly diverse, which limits the global model from maximizing performance for each individual client. This heterogeneously distributed data across multiple clients is the primary motivation in utilizing personalized versions of federated learning. In this research, we implement algorithms that use personalized federated learning techniques such as clustering clients and utilizing temporary models for communication. Various hyperparameters - batch size, local communication rounds, number of clients - are adjusted to maximize the algorithm's accuracy levels. The algorithms are implemented using PyTorch (a machine learning library developed by Facebook's AI Research Lab) and both trained and tested using the CIFAR-10 image dataset. Using random heterogeneously distributed data, the algorithms converge to higher accuracy levels through these personalization techniques when compared to traditional federated learning utilizing a singular global model. Personalized federated learning is a key component within future machine learning applications - such as connecting autonomous vehicles - as it combines the effectiveness of traditional machine learning with crucial cloud security and data privacy protection.

UCLA Samueli School of Engineering

SUMMER UNDERGRADUATE RESEARCH PROGRAM

A PERSONALIZED APPROACH TO FEDERATED LEARNING

Tyler Xu, Kaan Özkara[DLS], Suhas Diggavi[PI]
Information Theory and Systems Laboratory (Licos)
Department of Electrical and Computer Engineering, University of California – Los Angeles

Research Experiences for Undergraduates
National Science Foundation

FAST TRACK TO SUCCESS
UCLA Electrical and Computer Engineering

Introduction

Problem

Federated learning struggles with non-IID (non-idependent and identically distributed) diverse datasets due to its reliance upon a singular global model for multiple clients (devices). This traditional strategy is limited, as one global model cannot maximize the testing accuracy for different sets of data.

Approach

Implement personalized federated learning algorithms.
Personalized techniques (client clustering and utilizing temporary models) will result in algorithms converging to higher accuracy levels.

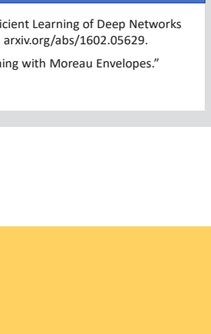

Materials and Methods

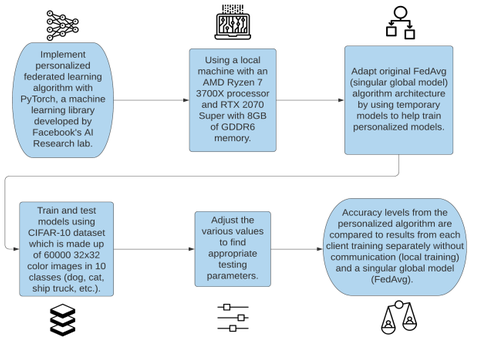

Results and Discussion

Setting batch size to 50, local epochs to 20, and number of clients to 6, the hyperparameters of regularization (reg) and learning rate levels are adjusted to achieve the optimized accuracy for the personalized (pFedMe) federated learning algorithm.

FedAvg Individual Client Model (IID)	FedAvg Global Model (non-IID)	pFedMe Personal Model (non-IID)
73%	49%	79%

Learning rate of 0.01 and regularization of 20 converges to the highest testing accuracy rate of 79% for the personalized algorithm.
A lower regularization is too slow to converge, while a high regularization will diverge.

	Reg 30	Reg 20	Reg 15	Reg 10	Reg 5
Learning Rate 0.01	76%	79%	78%	77%	74%
Learning Rate 0.05	71%	75%	74%	72%	70%

Conclusions

Personalized federated learning algorithms allow for models to outperform traditional federated learning algorithms when using non-IID data. Future implementation of other personalized algorithms such as FedFomo will further showcase the advantages of personalization techniques.

These techniques are key components within future machine learning applications (autonomous vehicles, traffic predictions, etc.) as they increase the performance of machine learning models on heterogenous datasets while eliminating data security risks within the cloud.

References

McMahan, H. Brendan, et al. "Communication-Efficient Learning of Deep Networks from Decentralized Data." ArXiv.org, 28 Feb. 2017, arxiv.org/abs/1602.05629.

Dinh, Canh T., et al. "Personalized Federated Learning with Moreau Envelopes." ArXiv.org, 3 Mar. 2021, arxiv.org/abs/2006.08848.

Acknowledgements

I would like to thank Kaan Özkara and Suhas Diggavi for their guidance and resources throughout this project. I would also like to thank NSF (REU) for their funding and the UCLA Summer Undergraduate Research Program (SURP) for this research opportunity.

Lime Yao

Computer Engineering
Freshman, UCLA

Courtney Gibbons

Electrical Engineering
Freshman, UCLA

Verifying Conditions for Magnetic Alignment in Canine Urination and Defecation with Citizen Science Dataset

FACULTY ADVISOR

Clarice Aiello

DAILY LAB SUPERVISOR

João Carlos Ribeiro-Silva

DEPARTMENT

Electrical and Computer Engineering

ABSTRACT

Numerous species of animals are known to have magnetoreception, or the ability to detect the Earth's magnetic field, for orientation and navigation. However, more research is needed to confirm the underlying mechanics of magnetoreception in animals. Compelling evidence has suggested that dogs align to the Earth's magnetic field during excremental activity if the nearby magnetic field declination, or the difference between true north and magnetic north, is stagnant. Nonetheless, this phenomenon needs a robust source of experimental data before it can be established. We are compiling a large image dataset of urinating and defecating dogs with citizen science and automating the analysis of geomagnetic metadata embedded within these images. We hope to verify whether canine alignment in urination and defecation depends on magnetic field declination. Initial results from a low sample size indicate dogs face random directions even when the percent change magnetic field declination is less than 1%. However, the project will require more image submissions from across the world to yield more refined results. If dogs demonstrate magnetoreception in the course of this project, their potential role as experimental subjects will be pivotal in developing future magnetoreception research.

UCLA Samueli School of Engineering

Previous research suggests **dogs align** with the **Earth's magnetic field** when they **urinate and defecate** if the **magnetic field declination** is **stagnant** at that point in space and time.

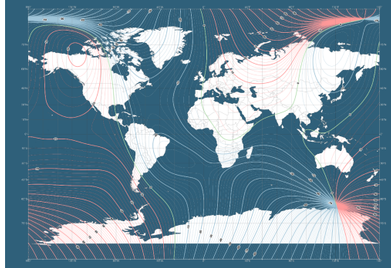

World magnetic model of main field declination, the difference between true North and magnetic North, in 2020 [2]. The green curves represent 0 magnetic field declination; the red curves represent positive magnetic field declination, indicating magnetic north is east of true north; and the blue curves represent negative magnetic field declination, indicating magnetic north is west of true north. The thicker curves occur every 10° magnetic north and true north vary from each other.

We seek to establish or refute this fact by **increasing the sample size** with **citizen science** and deploying **metadata extraction** and **automated analysis**.

Scan this to view our website & submit your dog photos!

Verfiying Conditions for Magnetic Alignment in Canine Urination and Defecation with Citizen Science Dataset

Courtney A. Gibbons, Lime Yao, Gina Talcott, Josh Cielo, Greg Damelin, Clarice D. Aiello
Department of Electrical and Computer Engineering, University of California – Los Angeles

Important Concepts

- **Magnetoreception:** the ability to detect the Earth's magnetic field.
- **Magnetic field declination:** the difference between true north and magnetic north.
- **Exif metadata:** information embedded in an image, such as geolocation and camera specifications.
- **Citizen science:** when the general public participates in scientific research, often by providing data.

Researching Magnetoreception in Dogs

- Previous research suggests **dogs have magnetoreception** and **align with the Earth's magnetic field during excremental activity** when the **magnetic field declination is stagnant** [1].
- With a sample size of only 70 dogs located in rural parts of Germany and the Czech Republic, **more research and data is needed** [1].
- We aim to expand the sample size by **compiling a large image dataset** of urinating and defecating dogs with **citizen science** and analyzing the **geomagnetic metadata** embedded within these images.
- We hope to **verify whether canine alignment in urination and defecation depends on magnetic field declination and environment.**

Fully Automated Image Collection Process

- We asked dog owners to take pictures **from behind their dog**, effectively **measuring the dog's magnetic orientation** like a compass would, when their dog was urinating or defecating.

Lab Social Accounts & Website
Obtain images of urinating & defecating dogs from participating dog owners.

Google Script
Sort photos based on environmental keywords.

Exif Metadata Extraction
Retrieve photo direction & GPS data.

Calculate Magnetic Field Declination
Use GPS data & NOAA calculator [2].

Analysis
Average direction across all dogs and correlate various factors that encourage or discourage magnetic alignment:
- Magnetic declination change
- Rural vs urban environment

UCLA Samueli School of Engineering SUMMER UNDERGRADUATE RESEARCH PROGRAM
FAST TRACK TO SUCCESS UCLA Electrical and Computer Engineering
uBiT

Preliminary Results with a Low Sample Size

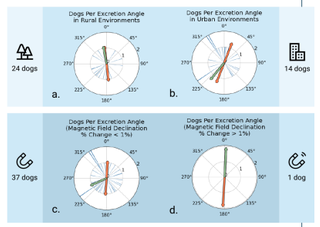

- Circular bar plots of **excretion angles east of north** are sorted by **rural (a)** versus **urban environments (b)** and **rate of magnetic field declination change below (c)** and **above (d) %1**.
- **Red vectors** indicate **average excretion axis**, and **green vectors** indicate **average excretion direction**. Vector **magnitudes** represent the **extent of dogs' preference for magnetic alignment** towards that direction.
- This preliminary data consisted of only 38 dog images, and the dogs of the current dataset exhibited **no preference for a particular angle** and faced in random directions.

Future Prospects and Simulations

- This project will require **more image submissions from across the world** to yield more refined results.
- **Simulated plots** indicate the desired result of this project: data from many dogs that allow us to **establish or refute if dogs align with the Earth's magnetic field when they urinate and defecate**.
- Other future prospects include:
  - **Update plots on our website** every time a new photo is submitted
  - **Engage the community** by featuring dogs that have contributed to our study
- If dogs demonstrate magnetoreception in the course of this study, their potential role as experimental subjects will be pivotal in developing **future magnetoreception research**.

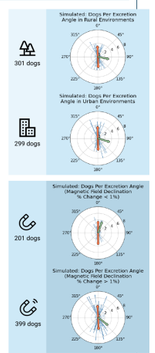

References and Acknowledgements

[1] Hart et al.: Dogs are sensitive to small variations of the Earth's magnetic field. Frontiers in Zoology 2013 10:80

[2] NCEI Geomagnetic Calculators: Magnetic Delincation Estimated Value. National Oceanic and Atmospheric Administration. https://www.ngdc.noaa.gov/geomag/ calculators/magcalc.shtml

We would like to thank the National Science Foundation (NSF), the UCLA Summer Undergraduate Research Program (SURP), and the UCLA Fast Track to Success program for this research opportunity. We also thank Professor Clarice Aiello for her knowledge and support.

Justin Yao

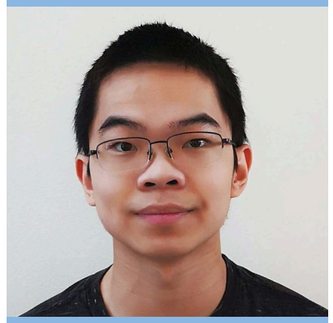

Electrical Engineering
Freshman, UCLA

Isabella Jordan

Electrical Engineering
Freshman, UCLA

Quantifying the Kerr Rotation Angle from the Magneto-Optic Kerr Effect of CoFeB and GdFeCo Films

FACULTY ADVISOR

Kang Wang

DAILY LAB SUPERVISOR

Bingqian Dai

DEPARTMENT

Electrical and Computer Engineering

ABSTRACT

We explored the magneto-optic Kerr effect (MOKE), which refers to the changes in light reflected from a magnetized surface. In MOKE, the incident circular polarized light becomes elliptically polarized and its axis of polarization rotates after reflection. These changes are termed Kerr ellipticity and Kerr rotation angle, respectively. Our objective is to achieve milli-radian Kerr rotation angle readout resolution on ferro/ferrimagnetic materials, such as CoFeB and GdFeCo, with a MOKE setup at near-normal incidence. By modulating the incident light with a photoelastic modulator (PEM-100), magnetizing the sample by placing it between two solenoids, and extracting voltage signals from a photo-detector with a lock-in amplifier (SR830) and multimeter (Keithley 2000), a magnetic hysteresis loop relating applied magnetic field strength and Kerr rotation angle was generated using MATLAB. The CoFeB sample was a wedge, meaning its thickness changed linearly from 0.4 to 1.4 nm. For this CoFeB wedge, we observed many hysteresis loops along the wedge to find both quantitative Kerr rotation angle and perpendicular magnetic anisotropy at various thicknesses. The GdFeCo film was of uniform thickness, but of a nonuniform makeup as it was a composition gradient from one side being Gd-rich and the other being FeCo-rich. For the GdFeCo film, the loops generated near the Gd-rich side neared but did not reach indication of a magnetization compensation point (where the net magnetic moment is 0). Points around the middle of the film were dominated by out-of-plane anisotropy, and the FeCo-rich side displayed predominantly in-plane anisotropy.

Quantifying the Kerr Rotation Angle from the Magneto-Optic Kerr Effect of CoFeB and GdFeCo Films

UCLA Samueli School of Engineering
SUMMER UNDERGRADUATE RESEARCH PROGRAM

Justin Yao and Isabella Jordan
Professor Wang, Bingqian Dai, Hanshen Huang
Department of Electrical and Computer Engineering

NSF FAST TRACK TO SUCCESS
UCLA Electrical and Computer Engineering

Introduction and Background

Magneto-Optic Kerr Effect

The magneto-optic Kerr effect (MOKE) refers to the changes in light reflected from a magnetized surface.

These changes primarily involve Kerr rotation angle, Kerr ellipticity, and intensity.

Name	(a) Polar	(b) Longitudinal	(c) Transverse
Geometry			
Detection	Out-of-plane	in-plane	in-plane
Polarization Variation	Rotation Ellipticity		None
Measurement	Polarization Analysis		Intensity measurement

Figure 1: The geometries of MOKE and the changes they introduce to incident light

Previous Work and Goals

The limitations of measuring MOKE stem from the extremely small changes that the effect produces, generally below 0.1 degrees. Previous research has explored all geometries of MOKE over a wide range of magnetic materials.

Our objective is to achieve milli-radian Kerr rotation angle readout resolution on ferro/ferrimagnetic materials, such as CoFeB and GdFeCo, with a MOKE setup at near-normal incidence.

Materials and Methods

Experimental Setup

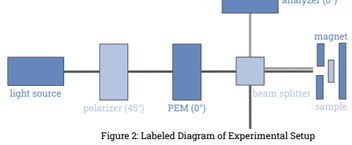

Figure 2: Labeled Diagram of Experimental Setup

Data Collection

1. Adjust the Sample Position
   The CoFeB wedge sample has linearly changing thickness (0.4-1.4 nm) along its length, and the GdFeCo is a composition gradient along its length. Adjusting where the beam shines on the sample produces a different result.
2. Align the Laser and Equipment
   Angle the sample in the magnet so that the laser reflects to the beam splitter at its brightest. Line up the analyzer and detector with the reflected beam until the lock-in amp reads a steady voltage
3. Run the Matlab Program
   Run the Matlab program that causes a current sweep from a max to min value at a designated step. A text file containing all the pertinent measurements will be saved.
4. Graph the Data
   Using a graphing software, graph Kerr rotation angle (of which the formula is given below) vs magnetic field.

$$\theta_k = \frac{\sqrt{2}}{4J_2}\frac{V_{2f}}{V_{DC}}$$

θ_k = Kerr rotation angle
V_{2f} = PEM 2nd harmonic
V_{DC} = DC signal
J_2 = Bessel function coeff.

References

https://www.researchgate.net/figure/Illustration-of-the-polar-magneto-optical-Kerr-effect-MOKE-Linearly-polarized-light_fig1_318002760
https://www.hindsinstruments.com/techniques/moke/

Results

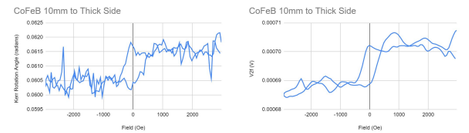

Figure 3: Magnetic hysteresis loops for the CoFeB wedge sample at 10mm to the thick side from the center. Left displays Kerr rotation angle, right displays V_{2f} for comparison

Figure 3 showcases the out-of-plane anisotropy of the CoFeB wedge sample, as there are two states of Kerr rotation angle corresponding to the two magnetization states. It is worth noting there is noise present in both graphs. In the Kerr rotation angle calculation, the ratio V_{2f}/V_{DC} is meant to eliminate drift or noise from the V_{2f} signal, but the V_{DC} signal itself has noise.

Figure 4: Magnetic hysteresis loops for the GdFeCo composition gradient sample, with one side being Gd-rich and another being CoFe-rich. Length measurements are taken from the center.

The GdFeCo sample had some unexpected results along its length. Figure 4 showcases the most prominent of these oddities, where out of plane anisotropy that is extremely similar to the CoFeB is displayed 10 mm towards the Gd-rich side instead of on the CoFe-rich side. Similarly, the magnetization compensation point, which should be in the middle of the sample, did not show, but 25mm towards the Gd-rich side, which is nearing the edge of the sample, a magnetic hysteresis loop bearing some resemblance to what would normally indicate a magnetization compensation point shows.

Conclusions and Future Prospects

Generating the CoFeB sample's hysteresis loops was more demonstrative as it showcased perpendicular magnetic anisotropy and verified the functionality of our setup. However, the GdCoFe sample and the data collected was far more unexpected. We attribute the irregular behavior to the sample, and suspect that the Gd was at no point dominant over the CoFe, and in the future we would certainly like to examine a GdCoFe sample with a centered magnetization compensation point

Ultimately, the data presented here possesses a signal to noise ratio doesn't quite meet the standard we had hoped for. We have a proposed solution that unfortunately the timescale of this project did not allow for, which was to doubly modulate the light with an optical chopper, then add a lock-in amplifier to read V_{DC} with significantly less noise.

Acknowledgements

We would like to thank the National Science Foundation for funding this research project and UCLA ECE Fast Track for the organization of this experience. Finally, we would like to thank Professor Kang Wang, Bingqian Dai, Hanshen Huang and the Device Research Laboratory for giving us this opportunity and their patience, mentorship, and support.

Ivy Zhang

Electrical Engineering
Freshman, UCLA

Tiffany Tsou

Electrical Engineering
Freshman, UCLA

Solving Large-Scale Non-metric Multidimensional Scaling Problems Using ADMM Optimization

FACULTY ADVISOR

Lieven Vandenberghe

DAILY LAB SUPERVISOR

Xin Jiang

DEPARTMENT

Electrical and Computer Engineering

ABSTRACT

Analysis of the relative orderings of the differences between model predictions as opposed to a quantitative method is often required in cases such as customers expressing their preferences instead of giving numerical scores. The purpose of this research project is to use an algorithm based on the alternating direction method of multipliers (ADMM) to solve large-scale non-metric multidimensional scaling (NMDS) problems. The NMDS problem seeks to optimize the Gram matrix of the calculated position vectors by minimizing violations of the inequality constraints that express the ordering relations of their pairwise distances. ADMM is a method for large-scale optimization which splits variable x into two parts and performs alternating optimizations over each part. The problem is coded using Python and Matlab, allowing us to see what fraction of the ordering of the original distances is preserved. We are working with randomly generated datasets. We are also working with more interesting data, including Swiss Roll and S curve data generated using Python, and real-world data such as sets of related images. For our initial results, which did not include any code for ADMM, the fraction of the ordering of distances preserved was quite high, indicating that the relative ordering of the original distances was preserved overall.

UCLA Samueli School of Engineering

Solving Large Scale Non-metric Multidimensional Scaling Problems Using ADMM Optimization

Tiffany Tsou and Ivy Zhang
Professor Lieven Vandenberghe, Xin Jiang, Taylor Chung

Samueli Research Scholars

UCLA Samueli School of Engineering
SUMMER UNDERGRADUATE RESEARCH PROGRAM

INTRODUCTION + OBJECTIVE

The goal of this research project is to use an algorithm based on the alternating direction method of multipliers (ADMM), to solve large-scale non-metric multidimensional scaling (NMDS) problems with randomly generated datasets and more interesting and real-world datasets such as the Swiss roll, S curve, and related images. Our hypothesis is that the calculated Gram matrix will preserve the ordering of the original distances between points in our initial dataset.

PRINCIPLES

NMDS: attempts to preserve the original distances between inputs in a dataset.
ADMM: a method for large-scale optimization which performs alternating optimizations over two vector variables x and y.
Convex optimization: a convex objective function is subject to inequality constraints that are summarized by a slack variable that we seek to minimize.

Figures: S curve and Swiss roll.

Source: https://www.semanticscholar.org/paper/Nonlinear-Manifold-Learning-6-.-454-Summary-Ihler/62bc7f7507f8f3e7c9c4ac62215d31b06e45da98/figure/0

MATERIALS

Python: Optimization package cvxpy
Matlab: Optimization package CVX
Datasets: Random datasets of size 50, Swiss roll dataset, S curve dataset, images

METHODS

1. Generate datasets with random data points, Swiss roll, S curve, images.
2. Code optimization problem along with ADMM solution into Python and then into Matlab.
3. Analyze results in Python and Matlab.
4. Make necessary adjustments to code and repeat.

$$\begin{aligned} \min_{K,\xi_{ijkl}} \quad & \sum_{(i,j,k,l)\in\mathcal{S}} \xi_{ijkl} + \lambda \operatorname{Trace}(K) \\ \text{subject to} \quad & k_{kk} - 2k_{kl} + k_{ll} - k_{ii} + 2k_{ij} - k_{jj} \geq 1 - \xi_{ijkl} \\ & \sum_{ab} k_{ab} = 0, \quad K \succeq 0. \qquad \text{(GNMDS)} \end{aligned}$$

This is the optimization problem with inequality constraints represented as linear equations of Gram matrix K which define a unique K which can solve the problem and have specifications that disallow translations, rotations, and scalings of K.
Source: Agarwal et al.

$$\begin{aligned} \text{minimize} \quad & \sum_{k=1}^{m} \max\{0, u_k\} + \lambda \mathbf{1}^T x + g(x) + h(y) \\ \text{subject to} \quad & \begin{bmatrix} I & 0 \\ 0 & I \end{bmatrix} \begin{bmatrix} x \\ u \end{bmatrix} + \begin{bmatrix} -I \\ -A \end{bmatrix} y = \begin{bmatrix} 0 \\ \mathbf{1} \end{bmatrix}. \end{aligned}$$

This is the optimization problem in an ADMM-ready form, which consists of first optimization over x and u, then optimization over y, and lastly the dual update. Source: Boyd et al.

RESULTS

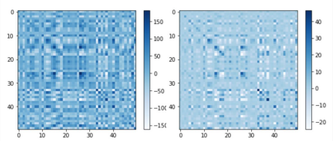

Figure: Shows the original Gram matrix calculated from the original distances matrix (left) and the calculated Gram matrix obtained by solving the non-metric multidimensional scaling problem (right).

Figure: Shows the values of the slack variable (error); ordering of distances is overall preserved.

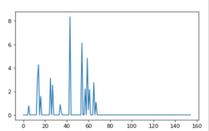

REFERENCES

Agarwal, S., Wills, J., Cayton, L., Lanckriet, G., Kriegman, D., & Belongie, S. (2007, March). Generalized non-metric multidimensional scaling. In Artificial Intelligence and Statistics (pp. 11-18). PMLR.
Boyd, S., Parikh, N., & Chu, E. (2011). Distributed optimization and statistical learning via the alternating direction method of multipliers. Now Publishers Inc.

ACKNOWLEDGEMENTS

We would like to thank the Summer Undergraduate Research Program for providing the guidance and resources to succeed with this project, Professor Lieven Vandenberghe, Xin Jiang, and Taylor Chung for providing their knowledge and resources, and NSF for funding this project.

David Zheng

Electrical Engineering
Freshman, UCLA

Serina Mummert

Physics
Sophomore, Citrus College

Flexible Prined Circuit Boards for Panofsky Quadrupole Electron Beam Guiding

FACULTY ADVISOR

Rob Candler

DAILY LAB SUPERVISOR

Benjamin Pound

DEPARTMENT

Electrical and Computer Engineering

ABSTRACT

Electron beam therapy (EBT) utilizes electrons to kill cancer cells with up to 60% less radiation affecting surrounding healthy tissue compared to photon-based radiation therapies. EBT typically uses cm-scale beams; this project focuses on using Panofsky quadrupoles to guide sub-millimeter beams in a flexible and changeable trajectory so that beam placement, and therefore treatment outcomes, are improved. Flexible Printed Circuit Boards (PCBs) were designed in a Panofsky quadrupole-like geometry, which consists of parallel copper traces that generate a quadrupolar magnetic field. The flexible material of the PCB allows for manipulation of electron beams in hard-to-reach areas for deeper tissue treatment. Joule heating of the PCBs was simulated in COMSOL Multiphysics, and the limiting current density extracted. The limiting current density was used in magnetostatic simulations to find the magnetic characteristics of these devices. Particle tracing simulations were then performed to investigate efficiency of guiding electrons at different curvatures of the flex-PCB. Flex PCBs were fabricated for testing and the thermal response of the PCBs was experimentally measured using a FLIR OnePro thermal camera.

UCLA Samueli School of Engineering

Flexible Printed Circuit Boards for Panofsky Quadrupole Electron Beam Guiding

Serina Mummert, David Zheng, Benjamin Pound, Professor Rob Candler
Department of Electrical and Computer Engineering, University of California -- Los Angeles

NSF UCLA Samueli School of Engineering SUMMER UNDERGRADUATE RESEARCH PROGRAM

Introduction

Flexible printed circuit boards were designed, simulated, and tested for potential use in **Electron Beam Therapy** (EBT) treatments.

EBT is a cancer treatment currently administered to patients around the world. It is highly effective and valued for its ability to treat tumors without causing excessive damage to surrounding healthy tissue. This makes EBT ideal for surface tumors, but treatment can improve with greater precision and control of electron beam placement.

Objectives

- Design smaller, cheaper, and easier to manufacture quadrupoles using Printed Circuit Board (PCB) technology.
- Test characteristics of these PCB quadrupoles to determine if they are feasible for use in real applications using simulations.
- Check if the quadrupoles still work even if they are bent.
- Measure thermal response with manufactured PCB designs.

Principles

Electrons are influenced by magnetic fields. This behavior is demonstrated in this research project using flexible printed circuit board (Flex-PCB) technology to induce magnetic fields via electric current. Flex-PCBs used as **Panofsky quadrupoles** guide electrons, focusing them in one axial direction.

A configuration of magnets as shown in Fig. 1 create a magnetic field focusing beams of charged particles.

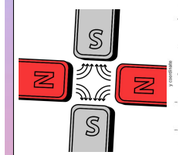

Figure 1: A quadrupole created by four permanent magnets with magnetic field direction.

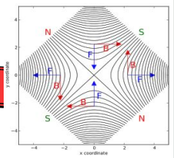

Figure 2: Magnetic force diagram of quadrupole configuration. Forces focus in vertical direction, and push away from the center in the horizontal direction.

Quadrupoles can be created using either permanent or electromagnets. Electromagnets are generally preferred as they are more easily controlled, allowing adjustment of the amount of current going through to achieve a desired magnetic field strength.

Quadrupole fields linearly vary with the distance from the beam axis. The field gradient of the quadrupole describes how fast the field strength changes with respect to distance from the center.
A higher value for this parameter means that particles feel a stronger force towards/away from the center.

Materials and Methods

01 CREATE A PCB DESIGN

- Determine magnetic properties of design using FEMM.
- Use Python to simulate electrons passing through multiple quadrupoles.
- Create Gerber files to send to the PCB factory for fabrication.

SIMULATE IN COMSOL MULTIPHYSICS 02

- Joule heating of PCBs was simulated and current density limits extracted.
- The limiting current density was used in magnetostatic simulations to find the magnetic characteristics of these devices.
- Particle tracing simulations were then performed to investigate efficiency of guiding electrons at different curvatures of the flex-PCB.

03 TESTING OUR DESIGNS

- PCBs were bought and tested with various amounts of current.
- Thermal response was recorded using FLIR OnePro thermal cameras.
- The results were compared to expected results from simulations.

Simulational Data

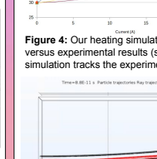

Figure 3: A cross sectional magnetic FEMM simulation of a flex-PCB Panofsky device with current running out of the page. The field lines are similar to that of an actual quadrupole.

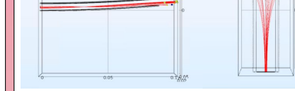

Figure 4: Our heating simulation results (shown by the colored lines) versus experimental results (shown by the data points). The simulation tracks the experimental results closely.

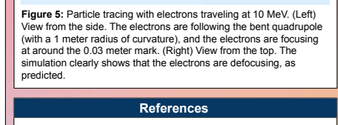

Figure 5: Particle tracing with electrons traveling at 10 MeV. (Left) View from the side. The electrons are following the bent quadrupole (with a 1 meter radius of curvature), and the electrons are focusing at around the 0.03 meter mark. (Right) View from the top. The simulation clearly shows that the electrons are defocusing, as predicted.

Test Results

Figure 6: The test setup used consists of a 12V power supply (1), a buck converter (2), steel wire as a variable resistor, (3) and a multimeter to measure current (4). The quadrupole being tested is at (5).

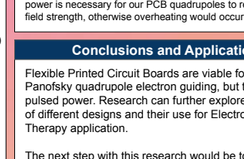

Figure 7: (Left) A picture of the quadrupole under test, with alligator clips to provide current. (Right): A picture of the same quadrupole but imaged with a thermal camera. The PCB is getting slightly warm in the picture.

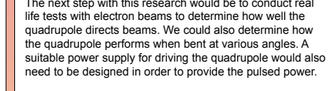

Figure 8: A plot of the temperature of the quadrupoles versus the amount of current passing through them. The temperature increases quadratically with respect to the current as predicted by Joule's Law of Heating. Due to outgassing, only a temperature increase of 10 degrees is allowed. The data shows that pulsed power is necessary for our PCB quadrupoles to reach the required field strength, otherwise overheating would occur with DC currents.

Conclusions and Applications

Flexible Printed Circuit Boards are viable for use in Panofsky quadrupole electron guiding, but they require pulsed power. Research can further explore the limitations of different designs and their use for Electron Beam Therapy application.

The next step with this research would be to conduct real life tests with electron beams to determine how well the quadrupole directs beams. We could also determine how the quadrupole performs when bent at various angles. A suitable power supply for driving the quadrupole would also need to be designed in order to provide the pulsed power.

In the future, better designs using thicker copper or using superconductors could be created to mitigate heating issues and allow for continuous operation without overheating. A separate cooling system using heat pipes to dissipate heat could also be used.

References

D. C. Meeker, Finite Element Method Magnetics, Version 4.2

Magnetic field of an idealized quadrupole with forces.svg. (2021, June 1). *Wikimedia Commons, the free media repository*.

Magnetic quadrupole moment.svg. (2020, September 27). Wikimedia Commons, the free media repository.

Acknowledgements

We appreciate the **National Science Foundation** for funding this research and thank the **UCLA SURP** for arranging this opportunity. We give special thanks to **Rob Candler** and **Benjamin Pound** for allowing us to assist with their great work.

SURP is an umbrella program that administers and scaffolds summer undergraduate research opportunities within UCLA Samueli Engineering. SURP participating sub-programs include National Science Foundation (NSF) Research Experience for Undergraduates (REU) Sites, Samueli Research Scholars (SRS) Program, Faculty-funded grants, and Electrical and Computer Engineering Fast Track Program.

William Herrera, the director of SURP, is also director of UCLA Samueli Engineering's Undergraduate Research and Internship Program (URP/UIP) during the academic year. URP/UIP is committed to helping you find research/internship opportunities. Our Peer Advisors are trained to help you with any questions and concerns you may have, and appointments are available on our website.

For any questions about these resources, please reach out to us at urp@seas.ucla.edu and uip@seas.ucla.edu, or scan the QR code on the next page to get to our website.

We also encourage you to follow us on social media to stay updated on future professional development event and opportunities.

seasoasa.ucla.edu/undergraduate-research-program/

Samueli Engineering Undergraduate Research and Internship Program

UCLA Samueli Undergraduate Internship Program

UCLA Engineering Internship and Research Program

samueliurpuip

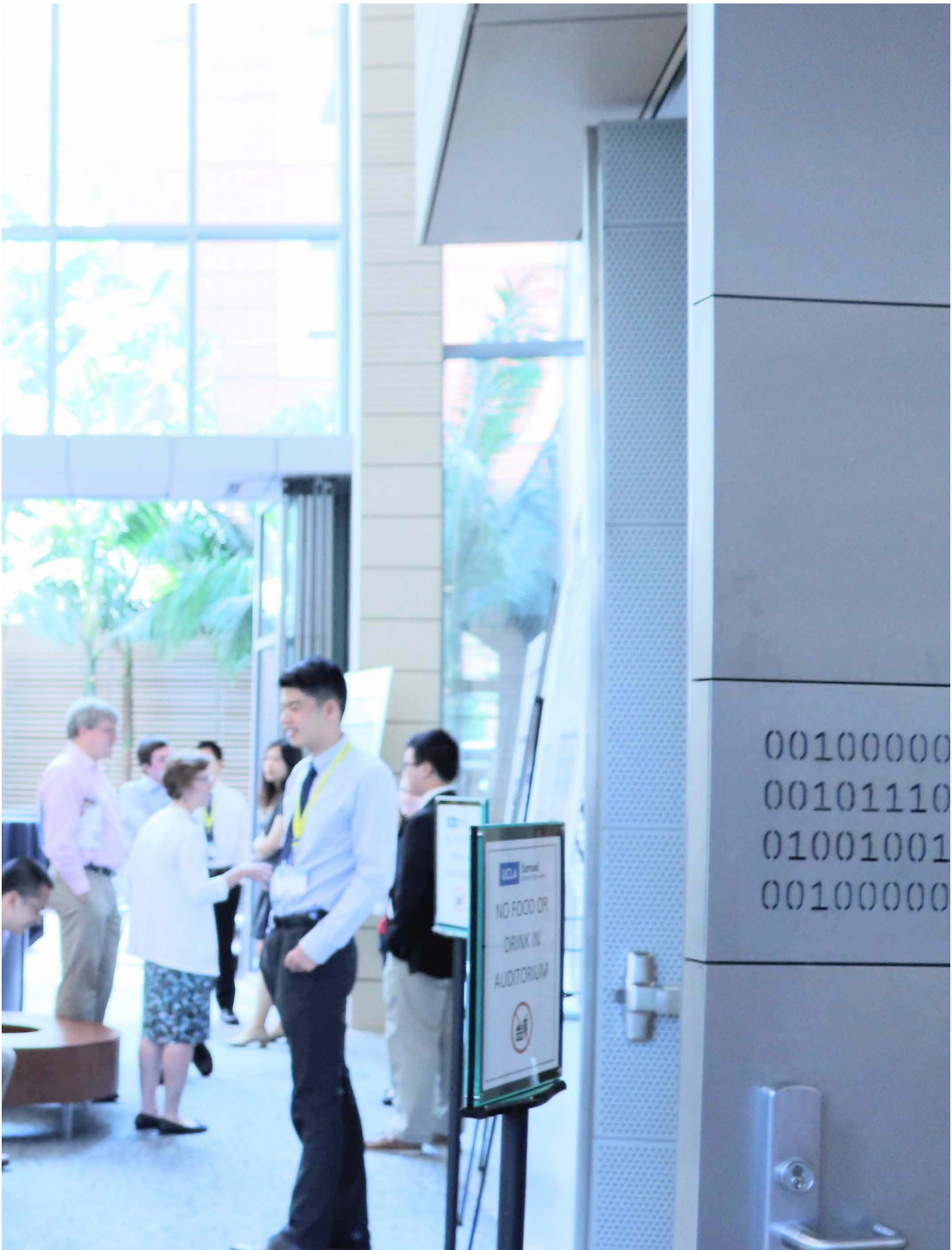
00100000
00101110
01001001
00100000
NO FOOD OR
DRINK IN
AUDITORIUM